



THE UNIVERSITY *of* EDINBURGH

Edinburgh Research Explorer

Neoplasms and novel gammaherpesviruses in critically endangered captive European minks (*Mustela lutreola*)

Citation for published version:

Nicolas de Francisco, O, Esperón, F, Juan-Sallés, C, Ewbank, AC, das Neves, CG, Marco, A, Neves, E, Anderson, N & Sacristán, C 2020, 'Neoplasms and novel gammaherpesviruses in critically endangered captive European minks (*Mustela lutreola*)', *Transboundary and Emerging Diseases*.
<https://doi.org/10.1111/tbed.13713>

Digital Object Identifier (DOI):

[10.1111/tbed.13713](https://doi.org/10.1111/tbed.13713)

Link:

[Link to publication record in Edinburgh Research Explorer](#)

Document Version:

Peer reviewed version

Published In:

Transboundary and Emerging Diseases

General rights

Copyright for the publications made accessible via the Edinburgh Research Explorer is retained by the author(s) and / or other copyright owners and it is a condition of accessing these publications that users recognise and abide by the legal requirements associated with these rights.

Take down policy

The University of Edinburgh has made every reasonable effort to ensure that Edinburgh Research Explorer content complies with UK legislation. If you believe that the public display of this file breaches copyright please contact openaccess@ed.ac.uk providing details, and we will remove access to the work immediately and investigate your claim.





Neoplasms and novel gammaherpesviruses in critically endangered captive European minks (*Mustela lutreola*)

Journal:	<i>Transboundary and Emerging Diseases</i>
Manuscript ID	TBED-OA-270-20.R1
Manuscript Type:	Original Article
Date Submitted by the Author:	23-Jun-2020
Complete List of Authors:	Nicolas, Olga; The University of Edinburgh Royal Dick School of Veterinary Studies Esperon, F.; CISA-INIA, Juan-Sallés, Carles; Noah's Path Ewbank, Ana; Universidade de Sao Paulo, Department of Pathology das Neves, Carlos; Norwegian Veterinary Institute Marco Valle, Alberto; Universitat Autònoma de Barcelona Facultat de Veterinària, Departament de Sanitat i d'Anatomia Animals Neves, Elena; CISA-INIA, Group of Epidemiology and Environmental Health Anderson, Neil; The University of Edinburgh Royal Dick School of Veterinary Studies Sacristán, Carlos; Universidade de Sao Paulo, Departamento de Patologia, Faculdade de Medicina Veterinaria e Zootecnia
Subject Area:	herpesvirus, lymphoma, mustelid, Conservation, Wildlife, Diagnostics, Virus

SCHOLARONE™
Manuscripts

1
2
3 **1 Neoplasms and novel gammaherpesviruses in critically endangered captive European**
4 **2 minks (*Mustela lutreola*)**

5
6
7 **3 Running title: Neoplasms and gammaherpesviruses in European minks**
8

9
10 4 Olga Nicolas de Francisco¹, Fernando Esperón², Carles Juan-Sallés³, Ana Carolina Ewbank⁴,
11 5 Carlos G. das Neves⁵, Alberto Marco⁶, Elena Neves², Neil Anderson¹ and Carlos Sacristán^{2,4,*}
12
13

14 6 ¹The Royal (Dick) School of Veterinary Studies and the Roslin Institute, University of
15 7 Edinburgh, Roslin, EH25 9RG, UK.

16
17
18 8 ²Group of Epidemiology and Environmental Health, Animal Health Research Center (INIA-
19 9 CISA).Valdeolmos, Madrid, 28130, Spain.

20
21
22 10 ³Noah's Path, Elche, Alicante, 03203, Spain.

23
24
25 11 ⁴Laboratory of Wildlife Comparative Pathology, Department of Pathology, School of Veterinary
26 12 Medicine and Animal Sciences, University of São Paulo, São Paulo, SP, 05508-270, Brazil.

27
28
29 13 ⁵Norwegian Veterinary Institute. Oslo, PO Box 750 Sentrum, Norway.

30
31
32 14 ⁶Departament de Sanitat i d'Anatomia Animals, Facultat de Veterinària, Universitat Autònoma
33 15 de Barcelona (UAB), Bellaterra-Barcelona, 08193, Spain.
34
35
36
37
38

39 17 *Corresponding author: Carlos Sacristán, Laboratory of Wildlife Comparative Pathology,
40 18 Department of Pathology, School of Veterinary Medicine and Animal Sciences, University of
41 19 São Paulo, São Paulo, SP, Av. Prof. Dr. Orlando Marques de Paiva, 87, 05508-270, Brazil; Tel:
42 20 +55 11 981 121 073; Email: carlosvet.sac@gmail.com
43
44
45
46
47
48
49
50
51
52
53
54
55
56
57
58
59
60

21 SUMMARY

22 The European mink (*Mustela lutreola*) is a riparian mustelid, considered one of the most
23 endangered carnivores in the world. Alpha, beta, and gammaherpesviruses described in mustelids
24 have been occasionally associated with different pathological processes. However, there is no
25 information about the herpesviruses species infecting European minks. In this study, 141 samples
26 of swabs (oral, conjunctival, anal), feces and tissues from 23 animals were analyzed for
27 herpesvirus (HV) using a pan-HV PCR assay. Two different, potentially novel,
28 gammaherpesvirus species were identified in 12 samples from four animals (17.3%), and
29 tentatively named Mustelid gammaherpesvirus-2 (MUGHV-2) and MuGHV-3. Gross
30 examination was performed ~~on~~ dead minks (n=11), while histopathology was performed ~~in~~
31 using available samples from HV-positive individuals (n=2), identifying several neoplasms,
32 including B-cell lymphoma (identified by immunohistochemistry) with intralesional syncytia and
33 intranuclear inclusion bodies characteristic of HV (n=1), pulmonary adenocarcinoma (n=1), and
34 biliary (n=1) and preputial (n=1) cystadenoma, as well as other lesions (e.g., axonal vacuolar
35 degeneration [n=2] and neuritis [n=1]). Viral particles, consistent with HVs, were observed by
36 electron microscopy in the mink with neural lymphoma and inclusion bodies. This is the first
37 description of neoplasms and concurrent gammaherpesvirus infection in European minks. The
38 pathological, ultrastructural and PCR findings (MuGHV-2) in the European mink with
39 lymphoma strongly suggest a potential role for this novel gammaherpesvirus in its pathogenesis,
40 as it has been reported in other HV-infected species with lymphoma. The occurrence of neural
41 lymphoma with intralesional syncytia and herpesviral inclusions is, however, unique among
42 mammals. Further research is warranted to elucidate the potential oncogenic properties of
43 gammaherpesviruses in European mink, and their epidemiology in the wild population.

44 **Keywords:** biliary cystadenoma, herpesvirus, lymphoma, lung adenocarcinoma, mustelid,
45 preputial cystadenoma.

46 INTRODUCTION

47 The European mink (*Mustela lutreola*) is a critically endangered riparian mustelid with
48 populations in eastern (Ukraine, Russia, Estonia and Romania) and western (south-western
49 France and northern Spain) Europe (Maran et al., 2016). The main factors causing its decline are
50 interspecies competition with the non-native American mink (*Neovison vison*), habitat loss and
51 degradation (pollution), over-hunting, and infectious diseases (e.g., Aleutian mink disease and
52 canine distemper) (Lodé et al., 2001; Maran et al., 2016; Mañas et al., 2016a). Without the
53 implementation of more effective conservation measures, the European mink will very likely
54 soon become extinct in Spain (Ferrer, 2014).

55 To date, the exposure to, and infection by, several viruses have been studied in wild European
56 minks: *Aleutian mink disease virus* (Mañas et al., 2001; Fournier-Chambrillon et al., 2004;
57 Guzmán et al., 2008; Mañas et al., 2016b), *Canine morbillivirus* (syn. canine distemper virus)
58 (Mañas et al., 2001; Guzmán et al., 2008; Philippa et al., 2008), canine parainfluenza virus (syn.
59 parainfluenza virus type 5 or *Mammalian rubulavirus 5*), canine adenovirus (syn. *Canine*
60 *mastadenovirus A*), and viruses belonging to the families *Astroviridae*, *Picobirnaviridae*, and
61 *Parvoviridae* subfamily *Parvovirinae* (Bodewes et al., 2014). Nevertheless, in spite of the
62 numerous members of the family *Herpesviridae* of veterinary and public health significance
63 (Huff & Barry, 2003; Widén et al., 2012), to the authors' knowledge, there is no information
64 about herpesviruses (HVs) in European minks. The HVs infecting vertebrates (family
65 *Herpesviridae*) are further subdivided into three subfamilies: *Alphaherpesvirinae*,
66 *Betaherpesvirinae* and *Gammaherpesvirinae* (ICTV, 2017). In other mustelid species, for
67 example the sea otter (*Enhydra lutris*), HV-like intranuclear inclusion bodies along with HV-
68 compatible virions, and exposure to herpesvirus have been described (Reimer & Lipscomb,
69 1998; Goldstein et al., 2011). Alpha-, beta- and gammaherpesviruses (α -HVs, β -HVs, γ -HVs)
70 were identified in American martens (*Martes Americana*) with no mention to associated disease
71 (Dalton et al., 2017). Only γ -HV infection has been reported in other mustelids: in oral
72 ulcerations and plaques, and nasal secretions of sea otters (Tseng et al., 2012); in ulcerative skin
73 lesions of a captive fisher (*Martes pennanti*) (Gagnon et al., 2011); and in free-living European
74 badgers (*Meles meles*) (Banks et al., 2002; Dandár et al., 2010, Sin et al., 2014), in which a γ -HV
75 has not yet been associated with lesions or clinical disease (King et al., 2004). Finally, the
76 susceptibility to α -HV *Suid alphaherpesvirus 1*, the etiological agent of Aujeszky'

1
2
3 77 disease/pseudorabies (Gorham et al., 1998; Quiroga et al., 1997; Liu et al., 2017; Wang et al.,
4 78 2018) and the replication of α -HV *Canine herpesvirus-1* in fetal lung cells (Reading & Field,
5 79 1999) have been reported in American mink.

8
9 80 The goals of this study were to: (1) survey if HVs are present in a European mink captive
10 81 population; and (2) describe the clinical and pathological findings with a particular focus on
11 82 morphological evidence of an association with herpesviral infection.

14 83 **MATERIALS AND METHODS**

15 84 **Study population and samples**

16 85 This study was performed on the captive European mink population of the Pont de Suert Captive
17 86 Breeding Center (Pont de Suert, Lleida, northeastern Spain) which is part of the Spanish
18 87 Breeding Program. Ethical approval for this study was granted by the R(D)SVS Veterinary
19 88 Ethical Review Committee (VERC, process number 57.17) and the Government of Catalonia
20 89 (Wildlife and Plant Service within the Department of Sustainability and Territory).

21 90 The European mink samples were obtained from the live animal collection of the Pont de Suert
22 91 captive collection in September 2017 (identified as LM = live mink) and from the dead mink
23 92 stored at that center until October 2017 (identified as PM = postmortem mink). All these mink
24 93 were either originated from Spanish captive breeding centers or captured in the wild, also in
25 94 Spain. Individual sex, last weight, date and place of birth (when available), origin, and arrival
26 95 date to Pont de Suert, and date of death or euthanasia are summarized in Appendix 1. All
27 96 European minks in Pont de Suert tested negative for *Aleutian mink disease virus* and *Canine*
28 97 *morbillivirus* antibodies upon their admission to the captive breeding program.

29 98 In September 2017, all live adult European mink in the breeding center were anesthetized for
30 99 routine health check with a combination of intramuscular ketamine (5 mg/kg, Imalgene 100
31 100 mg/mL, Merial Laboratorios SA, Barcelona, Spain) and medetomidine (0.1 mg/kg, Domtor,
32 101 Ecuphar Veterinaria SLU, Barcelona, Spain). Intramuscular atipamezole (0.1 mg/kg, Antisedan,
33 102 Zoetis SLU, Madrid, Spain) was used to reverse the effects of medetomidine a minimum of 20
34 103 minutes after anesthesia had been induced. All animals were individually placed back into their
35 104 cages after sampling and full recovery. During anesthesia, all mink received a full clinical
36 105 examination by an experienced veterinarian, which included body condition assessment, skin and
37 106 hair inspection for ectoparasites, abdominal palpation and general examination of the mucosae,

1
2
3 107 oral cavity, ears, anal-genital region and feet, and cardiac and pulmonary auscultation.
4
5 108 Approximately 2 ml of blood were withdrawn by venipuncture from the cranial vena cava using
6
7 109 21-gauge 3.8-cm needles for hematology, biochemistry (data not shown), and molecular analysis
8
9 110 (0.5 mL in a sterile eppendorf). Aside from 0.5 mL of whole blood, sterile oropharyngeal,
10
11 111 conjunctival and anal swabs were also collected for molecular analysis, and preserved frozen at -
12
13 112 20 °C. Fresh fecal samples were taken from the cages using a sterile tube and refrigerated for
14
15 113 direct observation and egg flotation techniques with zinc sulphate (33%) for endoparasite
16
17 114 detection (data not shown) or frozen (-20 °C) to perform viral DNA detection.

17 115 **Molecular diagnostics**

18
19
20 116 A total of 141 frozen tissue samples from 23 European minks were analyzed by PCR for HV
21
22 117 detection. Anal and conjunctival swabs, blood, and feces from live mink (n=12) and
23
24 118 representative tissue samples from carcasses (n=10) (Appendix 2) were submitted for PCR
25
26 119 analysis. One additional animal was sampled while alive and after its death (codes LM-9 and
27
28 120 PM-9), thus included in both categories (live animal and carcasses, Appendix 2). After a lysis
29
30 121 step with lysis buffer (Cell Signaling Technology, MA, USA), DNA extraction was performed
31
32 122 by pressure filtration (QuickGene DNA tissue kit S, FujiFilm Life Science, Tokyo, Japan).
33
34 123 Initially, a mediastinal neoplastic tissue mass from PM-1 (index case) was analyzed by a nested
35
36 124 pan-PCR that amplified a fragment of approximately 215-315 bp of the HV DNA polymerase
37
38 125 gene (VanDevanter et al., 1996). A second PCR was performed to amplify a 500 bp fragment of
39
40 126 the HV glycoprotein B gene for gammaherpesviruses (Ehlers et al., 2008). In order to explore the
41
42 127 presence of the novel HV sequence obtained from the neoplastic tissue, a comprehensive HV
43
44 128 screening in tissues and samples from the captive breeding center (both live and dead animals)
45
46 129 was performed using the PCR described by Ehlers et al. (2008). All glycoprotein B gene-positive
47
48 130 samples were also tested for herpesviral DNA polymerase gene (VanDevanter et al., 1996).

49
50 131 The PCR products of DNA polymerase and glycoprotein B were read-visualized in 1.5% agarose
51
52 132 gel stained with Red Safe® (Ecogen, Spain), and the amplicons of expected size were directly
53
54 133 sequenced with sequencing primers TGVseq and IYGseq (DNA polymerase), and 2760s and
55
56 134 2761as (glycoprotein B), respectively described by VanDevanter et al. (1996) and Ehlers et al.
57
58 135 (2008). The obtained sequences were compared to those previously published in GenBank using
59
60 136 a Blast search, and nucleotide (nt) and deduced amino acid (aa) p-distances were calculated with

1
2
3 137 MEGA Software 7.0 after editing out the primers (Kumar et al., 2016). After ClustalW alignment
4
5 138 of glycoprotein B gene nucleotide sequences by MEGA software 7.0 (Kumar et al., 2016), nt and
6
7 139 aa maximum likelihood phylogenetic trees were generated with 1000 bootstrap replicates,
8
9 140 including the newly identified HV sequences and 39 other α -, β -, and γ -HVs sequences. *Ictalurid*
10
11 141 *herpesvirus 1* was selected as an outgroup. Sequence information for members of the
12
13 142 *Herpesviridae* family was obtained from GenBank.

14 143 **Gross and microscopic examination**

15
16 144 Complete postmortem gross examination was performed in eleven European mink (identified
17
18 145 with codes PM-1 through PM-11). Eight of them (PM-2 – PM-8, and PM-10) were prominently
19
20 146 autolyzed. Microscopic evaluation was performed on HV-PCR-positive animals with adequate
21
22 147 tissue preservation (PM-1 and PM-9), using 10% formalin-fixed tissues embedded in paraffin,
23
24 148 sectioned at 5 μ m-thick, and stained with hematoxylin and eosin.

25 149 **Immunohistochemistry**

26
27 150 Immunohistochemical analyses were performed in 4 μ m-thick paraffin wax-embedded tissue
28
29 151 samples of PM-1 using antibodies against CD20 and CD3. Briefly, slides were transferred to a
30
31 152 PT-Link Automatic System of DAKO for deparaffinization, rehydration and epitope retrieval.
32
33 153 For this last step, slides were treated with acid buffer at pH 6 for 20 min. at 98°C, and then
34
35 154 transferred to distilled water. Endogenous peroxidase was then inhibited with Peroxidase-
36
37 155 Blocking Solution (from Dako, Ref.: S2023). Immunostaining was performed on a Dako
38
39 156 Autostainer Plus, using procedures, buffers and solutions provided by the fabricant. Briefly, as
40
41 157 first antibody, a polyyclonal Rabbit Anti- Human CD3 antibody (DAKO. Ref: A0452) and a
42
43 158 polyyclonal Rabbit Anti- Human CD20 antibody (CULTEK. Ref: PA5-32313) were both
44
45 159 incubated for 40 min. at room temperature, diluted 1:100 (CD3) and 1:200 (CD20) in
46
47 160 EnVision™ FLEX buffer. After washing, the Rabbit/Mouse EnVision Detection System (Dako
48
49 161 Ref.: K5007) was incubated at room temperature for 40 min, at the dilution recommended by the
50
51 162 [fabricantsupplier](#). After washing, slides were incubated for 5 min. in DAB-Chromogen-hydrogen
52
53 163 peroxide (Dako K3468), to reveal binding. After washing, slides were counterstained in Mayer's
54
55 164 haematoxylin for 10 seconds, washed in running tap water, and then automatically dehydrated,
56
57 165 cleared and mounted.

56 166 **Electron microscopy**

1
2
3 167 Transmission electron microscopy (TEM) was performed in a paraffin-embedded sample of a
4
5 168 perineural mass found in PM-1. The tissue sample was deparaffinized with histoclear,
6
7 169 dehydrated with 100% ethanol, infiltrated with LRWhite, sectioned into 60 nm sections and
8
9 170 contrasted with uranylacetate. Micrographs were obtained using a FEI Morgagni 268
10
11 171 transmission electron microscope and images were recorded by a side-mounted Olympus Veleta
12
13 172 CCD charge-coupled device camera.

14 173 **RESULTS**

15 174 **Molecular study**

16
17
18 175 Herpesvirus DNA was detected in four (PM-1, PM-4, PM-8, and LM/PM-9) out of the 23
19
20 176 evaluated European minks. Positive HV amplification was observed in 8.5% (12/141) of the
21
22 177 analyzed samples, including 11 from postmortem tissue samples and one from an antemortem
23
24 178 oral swab (LM/PM-9) (Appendix 2).

25
26 179 Two different glycoprotein B gene sequences were detected in the four HV-positive European
27
28 180 mink; one sequence was amplified from PM-1 (mediastinal mass) and PM-8 (lung), and a
29
30 181 different one from PM-4 (liver, kidney, brain), and LM/PM-9 (an antemortem oral swab, brain,
31
32 182 spinal cord, peripheral nerve [sciatic nerve and brachial plexus], spleen, and bone marrow). The
33
34 183 nt and aa identities between both novel glycoprotein B sequences were 79.9% and 86.0%,
35
36 184 respectively. The first sequence, found in PM-1 and PM-8, was more similar to the sequence
37
38 185 detected in a European badger (MuGHV-1, GenBank Accession number: ABF15169) with,
39
40 186 correspondingly, nt and aa identities of 87.2% and 97.8%. The second sequence, found in PM-4
41
42 187 and LM/PM-9, was more related to *Lynx rufus* gammaherpesvirus-2 (ABF15169), with nt
43
44 188 identity of 78.4%, and had the highest aa identity (86.0%) with a γ -HV identified in a harp seal
45
46 189 (KP136799). A phylogenetic tree based on glycoprotein B amino acid deduced sequences
47
48 190 correctly classified the two obtained novel sequences within the cluster of terrestrial mammal γ -
49
50 191 HVs, genus *Percavirus*, with bootstrap values above 70% (Figure 1).

51
52 192 A DNA polymerase sequence was amplified in one of the four HV-positive animals (PM-1),
53
54 193 while no amplification for that gene was observed in the remaining glycoprotein B gene-positive
55
56 194 cases. The highest nt (86.5%) and aa (92.2%) identities of this sequence were to the fisher
57
58 195 gammaherpesvirus (HM579931) obtained in another mustelid species, the fisher. The DNA
59
60 196 polymerase sequence of PM-1 was submitted to GenBank database under accession number

1
2
3 197 MN082678, while the glycoprotein B sequences obtained from PM-1 and PM-9 were submitted
4
5 198 under accession numbers MN082679 and MN082680, respectively. Since there was a previous
6
7 199 report using the terms “Mustelid gammaherpesvirus” (Mustelid gammaherpesvirus-1 or
8
9 200 MuGHV-1, Kent et al. [2018]), we have tentatively named the two novel sequences as MuGHV-
10
11 201 2 (PM-1 and PM-8) and MuGHV-3 (PM-4 and LM/PM-9). A summary of the γ -HVs detected in
12
13 202 mustelids is provided in Table 1.

14 203 **Retrieval of information prior to death or euthanasia of HV-positive mink**

15
16 204 Prior to death, PM-1 presented with corneal opacity in the left eye, protrusion of right eye, severe
17
18 205 incoordination, and rear limb weakness, leading to traumatic lesions and inability to eat. PM-4
19
20 206 presented with poor fur quality and compromised vision. PM-8 was uncoordinated and
21
22 207 eventually recumbent, which lead to a skin ulcer on its right hip. LM/PM-9 presented with
23
24 208 corneal opacity in the left eye and bilateral impaired vision, mild incoordination, rear limbs
25
26 209 weakness, and hyporexia that progressed to anorexia. In order to prevent suffering and based on
27
28 210 a full clinical examination and complementary examinations (hematology and biochemistry, data
29
30 211 not shown), two old animals (over nine years of age; PM-1 and LM/PM-9) were humanely
31
32 212 euthanized due to the rapid worsening of clinical signs.

32 213 **Gross and microscopic findings**

33
34 214 The gross and histopathologic findings of the HV-positive mink (PM-1, PM-4, PM-8 and
35
36 215 LM/PM-9) are summarized in Appendix 3. The main gross and microscopic findings and
37
38 216 suspected cause of death in PM-1 and LM/PM-9 are described below.

39
40 217 PM-1 was a 647-grams male with moderate to severe atrophy of adipose tissue. Protrusion of the
41
42 218 right eye due to the presence of a grayish to greenish retrobulbar mass involving the eyelid and
43
44 219 peri-ocular skin (Figure 2). The left eye had corneal opacity. Nerves in the left brachial plexus
45
46 220 and left elbow joint nerves were surrounded by whitish masses up to 1 cm in greatest dimension
47
48 221 (Figure 2). A similar but smaller lesion surrounded the right sciatic nerve distal to the
49
50 222 coxofemoral joint. A 5.5x2.8x2.2-cm whitish mass was also found in the caudal mediastinum
51
52 223 (Figure 2). The left adrenal gland was partly effaced by a grayish mass 1 cm in diameter (Figure
53
54 224 2).

55 225 Microscopically, all masses consisted of a malignant neoplastic proliferation of round cells

1
2
3 226 characterized by a round, oval, or more rarely irregular, indented or reniform nucleus with 1-2
4
5 227 nucleoli and diverse chromatin patterns, and a low amount of eosinophilic to amphophilic
6
7 228 cytoplasm. Anisocytosis, anisokaryosis, and anaplasia were moderate to high, while
8
9 229 pleomorphism was moderate. Up to 6 mitoses per 40x power field were observed. Neoplastic
10
11 230 cells invaded the perineurium and endoneurium of nerves within the masses (Figures 2 and 3).
12
13 231 Affected nerves contained large areas of necrosis with dilatation, vacuolation and fragmentation
14
15 232 of myelin sheaths as well as spheroids, deposits of fibrin, infiltrates of neutrophils and
16
17 233 lymphocytes, and foci of acute hemorrhage. Neural necrosis extended into the perineural
18
19 234 neoplastic tissue, where it was accompanied by prominent infiltration of degenerate neutrophils.
20
21 235 Neoplastic cells were present in the perineurium and endoneurium as well. Intralesional within
22
23 236 the endoneurium and neoplastic tissue, particularly in areas of necrosis, were syncytia and
24
25 237 intranuclear inclusion bodies. These inclusions were predominantly basophilic and filled the
26
27 238 nucleus, but eosinophilic inclusions surrounded by a clear halo were noted as well (Figure 3).
28
29 239 They were found within syncytia and, presumably, neoplastic cells. Similar infiltrates of
30
31 240 neoplastic cells along with fewer well differentiated lymphocytes and plasma cells were present
32
33 241 in the spinal cord and root nerves, involving the meninges with a diffuse pattern and neural tissue
34
35 242 with a perivascular and multifocal distribution. In the spinal cord, both the white and grey matter
36
37 243 was affected (Figure 3). Cerebral meninges were also mildly infiltrated, but predominantly with
38
39 244 well differentiated lymphocytes and plasma cells; neoplastic round cells were rare in this
40
41 245 location. Neoplastic infiltrates in the retrobulbar mass and adrenal gland caused loss of
42
43 246 architecture (Figure 2) and invaded adjacent soft tissues including the skin, adipose tissue and
44
45 247 skeletal muscle. Thrombosis was observed in the right eyelid. Other microscopic findings were
46
47 248 cataracts in left eye, axonal degeneration in a peripheral skeletal muscle nerve, nodular acinar
48
49 249 pancreatic hyperplasia, prostatic hyperplasia, moderate glomerulosclerosis. Additional gross and
50
51 250 microscopic findings are summarized in Appendix 3.

52
53 251 PM-9 was a 696-grams male in a good body condition. This mink presented corneal opacity in
54
55 252 left eye, and mild thickening of the nictitating membrane. A marked bilateral hemothorax was
56
57 253 present, and both lungs were multifocally reddish in color. A mass 0.5 cm diameter was observed
58
59 254 in the diaphragmatic lobe of the left lung. This mink had mild to moderate splenomegaly, with a
60
255 red splenic mass of 0.5 cm in diameter. A cystic mass 1.5 in diameter was also noted in the left
256
liver lobe. A subcutaneous preputial mass measuring 1x0.5x0.3 cm, and mild generalized

1
2
3 257 lymphadenomegaly were also observed. The adrenal glands contained pale foci less than 1 mm
4
5 258 in diameter.

6
7 259 Microscopically, the main disease processes and lesions included pulmonary adenocarcinoma,
8
9 260 severe membranous glomerulonephritis, severe chronic diffuse granulomatous lymphadenitis,
10
11 261 biliary cystadenoma, and preputial gland cell hyperplasia and cystadenomas with focal malignant
12
13 262 transformation and purulent preputial adenitis. Other potential relevant lesions included
14
15 263 moderate to marked meningeal mineralization in the lumbar and thoracic spinal cord, mild
16
17 264 multifocal spongiosis in the brain, axonal vacuolar degeneration in the thoracic spinal cord and
18
19 265 sciatic nerve, as well as nodular hyperplasia of adrenocortical cells, pancreatic acinar and ductal
20
21 266 cells and splenic tissue, mild multifocal fibrosis and/or interstitial lymphoplasmacytic nephritis
22
23 267 and glomerulosclerosis. Other gross and microscopic findings are summarized in Appendix 3.

23 268 **Immunohistochemical findings**

24
25 269 Positive immunolabeling for the B cell marker CD20 was consistently observed in neoplastic
26
27 270 cells in the perineural masses and endoneurium of intra-tumoral nerves (Figure 3). Labeling most
28
29 271 notably involved the membrane. No labeling of neoplastic cells was observed for CD3 (Figure
30
31 272 3). Therefore, the lymphoma was classified as a B-cell lymphoma.

32 273 **Transmission electron microscopy (TEM)**

33
34
35 274 Transmission electron microscopy detected particles approximately 150 nm in diameter in the
36
37 275 perineural lymphoma identified in PM-1 (Figure 4). Some of these were similar to empty
38
39 276 nucleocapsids while others resembled nucleocapsids containing packaged DNA, and both were
40
41 277 compatible with herpesviral particles (Ryner et al., 2006).

42 278 **DISCUSSION**

43
44
45 279 Two different novel γ -HV sequences were identified in 12 samples from four unrelated adult
46
47 280 captive European mink (17.3%, 4/23) that, based on amino acid identities and phylogeny, could
48
49 281 be considered novel HV species (MuGHV-2 and MuGHV-3). The prevalence rate should be
50
51 282 interpreted with care, once no housekeeping genes were amplified to test the integrity of the
52
53 283 DNA present in the samples. This is, to the authors' knowledge, the first report of HV in
54
55 284 European mink, expanding the host range of HV infections in mustelids. Other γ -HV species
56
57 285 have been previously described in mustelids (King et al., 2004, Tseng et al., 2012, Dalton et al.,

1
2
3 286 2017), occasionally identified in lesions such as oral ulcerations and plaques (Tseng et al., 2012),
4
5 287 and skin ulcers (Gagnon et al., 2011). Nevertheless, this is the first description of γ -HV
6
7 288 potentially associated with neoplasms in mustelids.

8
9 289 The two γ -HV-infected European minks with available tissues for histopathology (PM-1 and
10
11 290 LM/PM-9) had several neoplasms, including B-cell lymphoma (n=1), pulmonary
12
13 291 adenocarcinoma (n=1), biliary cystadenoma (n=1) and preputial cystadenoma (n=1). To the
14
15 292 authors' knowledge, these are the first neoplasms described in this species. Age and infectious
16
17 293 disease and inbreeding may have played a role in the development of neoplasm. The influence of
18
19 294 other factors that may also be implicated, such as environmental contamination or inbreeding,
20
21 295 was not assessed. In other carnivore species, for instance the California sea lion (*Zalophus*
22
23 296 *californianus*), collaborative studies showed that certain neoplasms (urogenital carcinoma) were
24
25 297 associated with genotype, but also with HV and persistent organic pollutants (King et al., 2002;
26
27 298 Browning et al., 2015).

28
29 299 In regard to age, both animals with neoplasms and HV-infection (PM-1 and LM/PM-9) were
30
31 300 considered to be of advanced age for the species (over nine years old). The oldest recorded free-
32
33 301 ranging European mink was five years old; however, captive animals can reach ten years of age
34
35 302 (Mañas et al., 2016a). The nodular acinar pancreatic hyperplasia, prostatic hyperplasia and
36
37 303 glomerulosclerosis observed in PM-1, as well as nodular acinar and ductal pancreatic
38
39 304 hyperplasia, and nodular splenic hyperplasia in LM/PM-9 were possibly related to aging. Aging
40
41 305 should be considered an immunosuppression factor per se (Marchioni & Berzero, 2015), capable
42
43 306 of facilitating neoplasm development.

44
45 307 The European mink with neoplasms - PM-1 and LM/PM-9 – were infected with
46
47 308 gammaherpesviruses MuGHV-2 and MuGHV-3, respectively. HV-compatible particles were
48
49 309 observed by TEM in a B-cell lymphoma with neural tissue tropism of PM-1, in which
50
51 310 intratumoral syncytia and intranuclear inclusion bodies characteristic of herpesviruses were
52
53 311 noted. Noteworthy, viruses have been associated with approximately 15% to 20% of human
54
55 312 cancers worldwide (Parkin et al., 2006; Boccardo & Villa, 2007). Several γ -HV are oncogenic
56
57 313 viruses. For instance, Epstein–Barr virus (*Human gammaherpesvirus 4*) has been etiologically
58
59 314 associated with a broad range of lymphoproliferative lesions and B-, T- and NK-cell malignant
60
315 lymphomas in humans (Shannon-Lowe et al., 2017), including B-cell lymphoma in elderly

1
2
3 316 populations, possibly associated with immunosuppression due to aging (El Jamal, 2014; Castillo
4 et al., 2016). Kaposi sarcoma-associated HV (syn. *Human gammaherpesvirus 8*) is associated
5 317 with Kaposi's sarcoma and lymphoproliferative disorders in humans (Du et al., 2007). In wild
6 318 mammals, γ -HVs have been implicated in the pathogenesis of several neoplastic diseases,
7 319 including urogenital carcinoma or multicentric B-cell lymphoblastic lymphoma in California sea
8 320 lion (Lipscomb et al., 2000; Venn-Watson et al., 2012; Browning et al., 2015).
9 321 Gammaherpesvirus-associated lymphoproliferative disease has been observed in captive non-
10 322 human primates of the family Callitrichidae (Ramer et al., 2000). The experimental inoculation
11 323 of γ -HV saimiri herpesvirus in three-striped night monkeys (*Aotus trivirgatus*) induced acute
12 324 lymphocytic leukemia (Melendez et al., 1971), while Epstein-Barr virus inoculation caused
13 325 lymphoma in cotton-top tamarins (*Saguinus oedipus*) (Miller et al., 1977). The herpesviruses
14 326 identified in both mink, particularly in PM-1, may have been involved in the etiopathogenesis of
15 327 the neoplasms found. Conversely, the detection of γ -HVs in several tissues from infected animals
16 328 presenting neoplasms could have been caused by viral reactivation from latency, triggered by,
17 329 among other causes, immunosuppression (which could be associated with the presence of
18 330 neoplasms), given that γ -HVs become latent in lymphoid cells (Roizmann et al., 1992).
19 331
20 332 In the domestic ferret, a species closely related to the European mink, lymphomas are common
21 333 spontaneous malignancies. Healthy ferrets experimentally inoculated with non-cellular extracts
22 334 from ferrets with lymphoma also developed this neoplasm, which reinforces the potential role of
23 335 infectious agents in the horizontal transmission of lymphomas in this species (Erdman et al.,
24 336 1995). The role of *Aleutian mink disease virus* and retrovirus infection has been suggested
25 337 (Erdman et al., 1992). Unfortunately, due to economic constraints, the potential role of
26 338 retroviruses in European minks has not been assessed yet.
27
28 339 Inbreeding is another factor that could partially explain the observed neoplasms. The French and
29 340 Spanish European minks appear to be highly inbred (Maran et al., 2016), and it would be
30 341 interesting to know if these highly genetically uniform populations are more prone to neoplasia.
31 342 For instance, the loss or lack of major histocompatibility complex (MHC) diversity, known to
32 343 reduce immune response effectiveness, is postulated to contribute to the successful spread of the
33 344 devil facial tumour disease of Tasmanian devils (*Sarcophilus harrisi*) (Siddle et al., 2007). The
34 345 association between neoplasm (urogenital carcinoma) and inbreeding has also been identified in
35 346 California sea lion (Acevedo-Whitehouse et al., 2003).

1
2
3 347 The neurological clinical signs – mainly incoordination and rear limb weakness, presented by
4
5 348 three of the four HV-positive animals (PM-1, PM-8, LM/PM-9, all over 9 years of age) were
6
7 349 initially considered typical signs of weakness or aging-related degenerative disorders. The
8
9 350 microscopic lesions described in the peripheral and central nervous systems of two of the
10
11 351 examined animals potentially explain the observed neurological signs: peripheral and central
12
13 352 nervous system B-cell lymphomas, axonal degeneration, and peripheral skeletal muscle nerves
14
15 353 axonal degeneration (PM-1), and brain spongiosis, and spinal cord and sciatic nerve axonal
16
17 354 vacuolar degeneration (LM/PM-9). The spongiosis and axonal degeneration observed in
18
19 355 LM/PM-9 could be associated with metabolic (e.g., renal encephalopathy) and/or toxic disorders.
20
21 356 Noteworthy, LM/PM-9 had severe glomerulonephritis, mild interstitial lymphoplasmacytic
22
23 357 nephritis, glomerulosclerosis and azotemia, with high urea (410 mg/dl) and creatinine levels
24
25 358 (1.44 mg/dl). These were elevated when compared with the reference values described in other
26
27 359 mustelid, the ferret: 11-42 mg/dl and 0.2-1 mg/dl, respectively (Carpenter & Marion, 2017) and
28
29 360 the remaining European minks analyzed in this study (data not shown), which could explain the
30
31 361 incoordination signs. No reference values are available for European mink.

32
33 362 Interestingly, the MuGHV-2 found in case PM-1 presented neural tissue tropism, with HV
34
35 363 particles observed in a perineural mass, and similarly, LM/PM-9 samples of brain, spinal cord,
36
37 364 peripheral nerve (sciatic nerve and brachial plexus) were positive to MuGHV-3. Both animals
38
39 365 had incoordination. The etiology of the neuritis in the B-cell lymphoma of PM-1 is unclear; it
40
41 366 could have been due to secondary inflammation associated with the local necrosis or a direct
42
43 367 response against herpesviral infection. Some γ -HVs have marked neurotropism, such as *Human*
44
45 368 *herpesvirus 4*/ Epstein–Barr virus and *Human herpesvirus 4*/Kaposi's sarcoma-associated HV
46
47 369 (KSHV) (El Jamal et al., 2014; Tso et al., 2016). For instance, Epstein–Barr virus has been
48
49 370 suggested to cause CNS damage by parainfectious and direct virus-related mechanisms in
50
51 371 humans (e.g., meningitis, encephalitis and lymphoma) (El Jamal et al., 2014). Thus, it is not
52
53 372 possible to exclude HVs as the potential causative agents of the nervous clinical signs observed
54
55 373 in these infected mink. Cataracts, corneal melanosis, focal granulomatous conjunctivitis in left
56
57 374 eye, and protrusion of and periocular mass around the right eye observed in PM-1 may have
58
59 375 contributed to its impaired vision. All mink were seronegative to two other viral agents that
60
376 could also cause neurological clinical signs and/or impaired vision: *Aleutian mink disease virus*
377 (Hadlow, 1982; Dyer et al., 2000), and canine distemper (Summers et al., 1984). Histopathologic

1
2
3 378 evidence of infection with *Toxoplasma gondii*, *Encephalitozoon* spp. or *Sarcocystis neurona* was
4
5 379 not observed.

6
7 380 One of the novel European mink γ -HVs (Mu-GHV3) was detected in an antemortem oral swab
8
9 381 (LM-9), suggesting that viral shedding occurs in infected European minks and, therefore, that
10
11 382 horizontal HV transmission through oral secretions could be possible. Such characteristic has
12
13 383 been previously identified in γ -HV viruses; Epstein–Barr virus is commonly transmitted via
14
15 384 saliva (Marchioni & Berzero, 2015), and other γ -HVs have been detected in sea otter oral
16
17 385 mucosal ulcers and plaques (Tseng 2012), and in oral tissue and swabs samples from northern
18
19 386 elephant seals (*Mirounga angustirostris*) (Goldstein et al., 2006). None of the mink in this study
20
21 387 has oral ulcers. Transmission can be enhanced in captivity as close confinement leads to a higher
22
23 388 contact rate between animals and stress-related immunosuppression (Tseng et al., 2012).
24
25 389 Interestingly, one of the infected European minks (LM/PM-9) had lesions compatible with
26
27 390 chronic stress (bilateral nodular hyperplasia of adrenocortical cells), which could reactivate latent
28
29 391 γ -HV in the lymphoid tissue (Roizmann et al., 1992; Lam et al., 2013).

30
31 392 Three of the HV-infected European minks were captured in the Ebro River basin (PM-4, PM-8
32
33 393 and LM/PM-9). The fourth one (PM-1) was born in Pont de Suert in 2006. Herpesvirus can cause
34
35 394 lifelong infections (Roizmann et al., 1992); therefore, it was not possible to establish if these
36
37 395 animals became infected during their stay in the captive breeding center (the virus was detected
38
39 396 when they had already been in captivity for several years) or already carried the virus when they
40
41 397 joined the collection. As several European mink conservation programs involving species
42
43 398 restoration and reintroduction use animals bred in captivity (Mañas et al., 2001), future studies
44
45 399 should investigate whether these HVs are present in wild European mink populations. Due to the
46
47 400 fact that several HV infections predispose the host to secondary bacterial infections (Cabello et
48
49 401 al., 2013), and considering the small size of the European mink population, the authors believe
50
51 402 that monitoring for these viruses should be considered when implementing conservation
52
53 403 strategies including translocations, as has been advised for other species, e.g., the Darwin's fox
54
55 404 (*Lycalopex fulvipes*) (Cabello et al., 2013).

51 405 **CONCLUSIONS**

52
53 406 This is the first report of HV in European minks. Four European minks were positive to one of
54
55 407 the two identified novel herpesviruses: *Mustelid gammaherpesvirus 2* (MuGHV-2) and *Mustelid*

1
2
3 408 *gamma*herpesvirus 3 (MuGHV-3). Several neoplasms, including B-cell lymphoma,
4
5 409 adenocarcinoma and biliary and preputial cystadenoma, as well as neurological signs, were
6
7 410 observed in some of the γ -HV-infected European minks. Aside from the B-cell lymphoma case
8
9 411 potentially associated with MuGHV-2, the relationship between γ -HV infection and the
10
11 412 remaining lesions is unclear.

12 413 This study contributes to the conservation of European minks by expanding the current
13
14 414 knowledge on the viral diseases affecting this species. Additional research is needed to establish
15
16 415 the prevalence of these novel γ -HVs in free-ranging European mink populations, and to
17
18 416 investigate their pathogenicity and the role of herpesvirus and other potential cofactors in the
19
20 417 neoplasms detected in this particular European mink captive breeding population. This
21
22 418 information will be critical to take more scientifically based decisions and adopt management
23
24 419 techniques for the conservation of this endangered species, as well as to determine if infected
25
26 420 captive bred European minks could be released into the wild without negatively impacting the
27
28 421 species' conservation.

28 422 **Acknowledgements**

29
30 423 We thank the Pont de Suert Captive Breeding Center staff for their assistance and for providing
31
32 424 data and audiovisual information on the studied animals and Lene C. Hermansen (Imaging
33
34 425 Center, Norwegian University of Life Sciences) for the TEM analysis. We also thank Francesc
35
36 426 Mañas (Department of Environment, Generalitat de Catalunya) and Madis Podra (European
37
38 427 Mink Association) for their support and interest in this project, and for providing the information
39
40 428 regarding the studied animals, and Francisco Fernandez Rivera, Head of the Environmental
41
42 429 management in Forestal Catalana, for authorizing this study. Ana Carolina Ewbank receives a
43
44 430 doctoral-fellowship from the São Paulo Research Foundation (FAPESP, process number
45
46 431 2018/20956-0). Carlos Sacristán is a recipient of a post-doctoral fellowship by the FAPESP
47
48 432 (process number 2018/25069-7). This study was funded by the Innovation Initiative Grant (IIG)
49
50 433 and by donors of the Edinburgh Fund (University of Edinburgh).

51 434 **Conflict of Interest Statement:** the authors declare no conflict of interest.

52 435 **Data Availability Statement:** The data that supports our findings are available in the manuscript
53
54 436 and in the supplementary material.

437 **REFERENCES**

- 438 Acevedo-Whitehouse, K., Gulland, F., Greig, D., & Amos, W. (2003). Inbreeding: disease
439 susceptibility in California sea lions. *Nature*, 422, 35. <https://doi.org/10.1038/422035a>
- 440 Banks, M., King, D. P., & Daniells, C. (2002). Partial characterization of a novel
441 gammaherpesvirus isolated from a European badger (*Meles meles*). *Journal of General Virology*,
442 83, 1325–1330. <https://doi.org/10.1099/0022-1317-83-6-1325>
- 443 Bodewes, R., Ruiz-Gonzalez, A., Schapendonk, C. M., van den Brand, J. M., Osterhaus, A.D., &
444 Smits, S. L. (2014). Viral metagenomic analysis of feces of wild small carnivores. *Virology*
445 *Journal*, 11, 89. <https://doi.org/10.1186/1743-422X-11-89>
- 446 Boccardo, E., & Villa, L. L. (2007). Viral origins of human cancer. *Current Medicinal*
447 *Chemistry*, 14, 2526–2539. <https://doi.org/10.2174/092986707782023316>
- 448 Browning, H. M., Gulland, F. M. D., & Hammond, J. A. (2015). Common cancer in a wild
449 animal: the California sea lion (*Zalophus californianus*) as an emerging model for
450 carcinogenesis. *Philosophical Transactions of the Royal Society B*, 370, 1673.
451 <https://doi.org/10.1098/rstb.2014.0228>.
- 452 Cabello, J., Esperón, F., Napolitano, C., Hidalgo, E., Dávila, J. A., & Millán, J. (2013).
453 Molecular identification of a novel gammaherpesvirus in the endangered Darwin's fox
454 (*Lycalopex fulvipes*). *Journal of General Virology*, 94, 2745–2749.
455 <https://doi.org/10.1099/vir.0.057851-0>.
- 456 Carpenter, J. W., & Marion, C. (2017). *Exotic Animal Formulary* (5th ed.). Philadelphia, PA:
457 Saunders.
- 458 Castillo, J. J., Beltran, B. E., Miranda, R. N., Young, K. H., Chavez, J. C., & Sotomayor, E. M.
459 (2016). EBV-positive diffuse large B-cell lymphoma of the elderly: 2016 update on diagnosis,
460 risk-stratification, and management. *American Journal of Hematology*, 91, 529-537.
461 <https://doi.org/10.1002/ajh.24370>
- 462 Dalton, C. S., van de Rakt, K., Fahlman, Å., Ruckstuhl, K., Neuhaus, P., Popko, R., Kutz, S., &
463 van der Meer, F. (2017). Discovery of herpesviruses in Canadian wildlife. *Archives of Virology*,
464 162, 449-456

- 1
2
3 465 Dandár, E., Szabó, L., & Heltai, M. (2010). PCR screening of mammalian predators (Carnivora)
4 466 for adenoviruses and herpesviruses: the first detection of a mustelid herpesvirus in Hungary.
5 467 *Magyar Allatorvosok Lapja*, 132, 302-308.
- 6
7
8 468 Du, M. -Q., Bacon, C. M., & Isaacson, P. G. (2007). Kaposi sarcoma-associated
9 469 herpesvirus/human herpesvirus 8 and lymphoproliferative disorders. *Journal of Clinical*
10 470 *Pathology*, 60, 1350-1357.
- 11
12
13
14 471 Dyer, N. W., Ching, B., & Bloom, M. E. (2000). Nonsuppurative meningoencephalitis associated
15 472 with Aleutian mink disease parvovirus infection in ranch mink. *Journal of Veterinary Diagnostic*
16 473 *Investigation*, 12, 159–162. <https://doi.org/10.1177/104063870001200212>
- 17
18
19
20 474 Ehlers, B., Dural, G., Yasmum, N., Lembo, T., de Thoisy, B., Ryser-Degiorgis, M. P., Ulrich, R.
21 475 G., & McGeoch, D. J. (2008). Novel mammalian herpesviruses and lineages within the
22 476 Gammaherpesvirinae: cospeciation and interspecies transfer. *Journal of Virology*, 82, 3509–
23 477 3516. <https://doi.org/10.1128/JVI.02646-07>.
- 24
25
26
27 478 El Jamal, S., Li, S., Bajaj, R., Wang, Z., Kenyon, L., Glass, J., Pang, C.S., Bhagavathi, S.,
28 479 Peiper, S. C., & Gong, J. Z. (2014). Primary central nervous system Epstein–Barr virus-positive
29 480 diffuse large B-cell lymphoma of the elderly: a clinicopathologic study of five cases. *Brain*
30 481 *Tumor Pathology*, 31, 265–273. <https://doi.org/10.1007/s10014-013-0173-x>
- 31
32
33
34 482 Erdman, S. E., Moore, F. M., Rose, F. M., & Fox, J. G. (1992). Malignant lymphoma in ferrets:
35 483 clinical and pathological findings in 19 cases. *Journal of Comparative Pathology*, 106, 37–47.
36 484 [https://doi.org/10.1016/0021-9975\(92\)90066-4](https://doi.org/10.1016/0021-9975(92)90066-4)
- 37
38
39
40 485 Erdman, S. E., Reimann, K. A., Moore, F. M., Kanki, P. J., Yu, Q. C., & Fox, J. G. (1995).
41 486 Transmission of a chronic lymphoproliferative syndrome in ferrets. *Laboratory Investigation; a*
42 487 *Journal of Technical Methods and Pathology*, 72, 539-546.
- 43
44
45 488 Ferrer, M. (2014). Life Lutreola Spain (2014-2018). Retrieved from
46 489 [http://ec.europa.eu/environment/life/project/Projects/index.cfm?fuseaction=search.dspPage&n_p](http://ec.europa.eu/environment/life/project/Projects/index.cfm?fuseaction=search.dspPage&n_proj_id=4908)
47 490 [roj_id=4908](http://ec.europa.eu/environment/life/project/Projects/index.cfm?fuseaction=search.dspPage&n_proj_id=4908)
- 48
49
50
51 491 Fournier-Chambrillon, C., Aasted, B., Perrot, A., Pontier, D., Sauvage, F., Artois, M., Cassiède,
52 492 J. M., Chauby, X., Dal Molin, A., Simon, C., & Fournier, P. (2004). Antibodies to Aleutian mink
53 493 disease parvovirus in free-ranging European mink (*Mustela lutreola*) and other small carnivores

- 1
2
3 494 from southwestern France. *Journal of Wildlife Diseases*, 40, 394-402.
4
5 495 <https://doi.org/10.7589/0090-3558-40.3.394>
6
7 496 Gagnon, C. A., Tremblay, J., Larochelle, D., Music, N., & Tremblay, D. (2011). Identification of
8
9 497 a novel herpesvirus associated with cutaneous ulcers in a fisher (*Martes pennanti*). *Journal of*
10
11 498 *Veterinary Diagnostic Investigation*, 23, 986–990. <https://doi.org/10.1177/1040638711418615>.
12
13 499 Goldstein, T., Lowenstine, L. J., Lipscomb, T. P., Mazet, J. A., Novak, J., Stott, J. L., & Gulland,
14
15 500 F. M., (2006). Infection with a novel gammaherpesvirus in northern elephant seals (*Mirounga*
16
17 501 *angustirostris*). *Journal of Wildlife Diseases*, 42, 830–835. [https://doi.org/10.7589/0090-3558-](https://doi.org/10.7589/0090-3558-42.4.830)
18
19 502 [42.4.830](https://doi.org/10.7589/0090-3558-42.4.830)
20
21 503 Goldstein, T., Gill, V. A., Tuomi, P., Monson, D., Burdin, A., Conrad, P. A., Dunn, J. L., Field,
22
23 504 C., Johnson, C., Jessup, D. A., Bodkin, J., & Doroff, A. M. (2011). Assessment of clinical
24
25 505 pathology and pathogen exposure in sea otters (*Enhydra lutris*) bordering the threatened
26
27 506 population in Alaska. *Journal of Wildlife Diseases*, 47, 579-592. [https://doi.org/10.7589/0090-](https://doi.org/10.7589/0090-3558-47.3.579)
28
29 507 [3558-47.3.579](https://doi.org/10.7589/0090-3558-47.3.579)
30
31 508 Gorham, J. R., Hartsough, G. R., & Burger, D. (1998). An epizootic of pseudorabies in ranch
32
33 509 mink. *Scientifur*, 22, 243-245.
34
35 510 Guzmán, D. S. M., Carvajal, A., García-Marín, J. F., Ferreras, M. C., Pérez, V., Mitchell, M.,
36
37 511 Urra, F., & Ceña, J. C. (2008). Aleutian disease serology, protein electrophoresis, and pathology
38
39 512 of the European mink (*Mustela lutreola*) from Navarra, Spain. *Journal of Zoo and Wildlife*
40
41 513 *Medicine*, 39, 305–313. <https://doi.org/10.1638/2006-0033.1>
42
43 514 Hadlow, W. J. (1982). Ocular lesions in mink affected with Aleutian disease. *Veterinary*
44
45 515 *Pathology*, 19, 5–15. <https://doi.org/10.1177/030098588201900103>
46
47 516 Huff, J. L., & Barry, P. A. (2003). B-Virus (*Cercopithecine herpesvirus 1*) infection in humans
48
49 517 and macaques: potential for zoonotic disease. *Emerging Infectious Diseases*, 9, 246-250.
50
51 518 <https://doi.org/10.3201/eid0902.020272>
52
53 519 ICTV (International Committee on Taxonomy of Viruses). (2017). Virus Taxonomy: The
54
55 520 Classification and Nomenclature of Viruses. Online (9th) Report of the ICTV. Email ratification
56
57 521 2017 (MSL #31). Retrieved from https://talk.ictvonline.org/ictv-reports/ictv_online_report/

- 1
2
3 522 Kent, A., Ehlers, B., Mendum, T., Newman, C., Macdonald, D. W., Chambers, M., & Buesching,
4 523 C. D. (2018). Genital tract screening finds widespread infection with Mustelid
5 524 Gammaherpesvirus 1 in the European badger (*Meles meles*). *Journal of Wildlife Diseases*, *54*,
6 525 133-137. <https://doi.org/10.7589/2016-12-274>
- 7
8
9
10
11 526 [King, D. P., Hure, M. C., Goldstein, T., Aldridge, B. M., Gulland, F. M., Saliki, J. T., Buckles,](#)
12 527 [E. L., Lowenstine, L. J., & Stott, J. L. \(2002\). Otarine herpesvirus-1: a novel gammaherpesvirus](#)
13 528 [associated with urogenital carcinoma in California sea lions \(*Zalophus californianus*\). *Veterinary*](#)
14 529 [Microbiology](#), *86*, 131-137. [https://doi.org/10.1016/s0378-1135\(01\)00497-7](https://doi.org/10.1016/s0378-1135(01)00497-7)
- 15
16
17
18 530 King, D. R., Mutukwa, N., Lesellier, S., Cheeseman, C., Chambers, M. A., & Banks, M. (2004).
19 531 Detection of Mustelid herpesvirus-1 infected European badgers (*Meles meles*) in the British
20 532 Isles. *Journal of Wildlife Diseases*, *40*, 99–102. <https://doi.org/10.7589/0090-3558-40.1.99>
- 21
22
23 533 Kumar, S., Stecher, G., Tamura, K. (2016). MEGA7: Molecular Evolutionary Genetics Analysis
24 534 version 7.0 for bigger datasets. *Molecular Biology and Evolution*, *33*, 1870–1874.
25 535 <https://doi.org/10.1093/molbev/msw054>
- 26
27
28
29 536 Lam, L., Garner, M. M., Miller, C. L. (2013). A novel gammaherpesvirus found in oral
30 537 squamous cell carcinomas in sun bears (*Helarctos malayanus*). *Journal of Veterinary Diagnostic*
31 538 *Investigation*, *25*, 99–106.
- 32
33
34 539 Lipscomb, T. P., Scott, D. P., Garber, R. L., Krafft, A. E., Tsai, M. M., Lichy, J. H.,
35 540 Taubenberger, J. K., Schulman, F. Y., & Gulland, F. M. (2000). Common metastatic carcinoma
36 541 of California sea lions (*Zalophus californianus*): evidence of genital origin and association with
37 542 novel gammaherpesvirus. *Veterinary Pathology*, *37*, 609–617. [https://doi.org/10.1354/vp.37-6-](https://doi.org/10.1354/vp.37-6-609)
38 543 [609](#)
- 39
40
41
42
43 544 Liu, H., Li, X. T., Hu, B., Deng, X. Y., Zhang, L., Lian, S. Z., Zhang, H. L., Lv, S., Xue, X. H.,
44 545 Lu, R. G., Shi, N., Yan, M. H., Xiao, P. P., & Yan, X. J. (2017). Outbreak of severe pseudorabies
45 546 virus infection in pig-offal-fed farmed mink in Liaoning Province, China. *Archives of Virology*,
46 547 *162*, 863-866. <https://doi.org/10.1007/s00705-016-3170-7>.
- 47
48
49
50 548 Lodé, T., Cormier, J. P., & Le Jacques, D. (2001). Decline in endangered species as an indication
51 549 of anthropic pressures: the case of European mink *Mustela lutreola* Western population.
52 550 *Environmental Management*, *28*, 727-735. <https://doi.org/10.1007/s002670010257>
- 53
54
55
56
57
58
59
60

- 1
2
3 551 Mañas, S., Ceña, J. C., Ruiz-Olmo, J., Palazón, S., Domingo, M., Wolfenbarger, J. B., & Bloom,
4 552 M. E. (2001). Aleutian mink disease parvovirus in wild riparian carnivores in Spain. *Journal of*
5 553 *Wildlife Diseases*, 37, 138-144. <https://doi.org/10.7589/0090-3558-37.1.138>
- 6
7
8 554 Mañas, S., Gómez, A., Asensio, V., Palazón, S., Pödra, M., Casal, J., & Ruiz-Olmo, J. (2016a).
9 555 Demographic structure of three riparian mustelid species in Spain. *European Journal of Wildlife*
10 556 *Research*, 62, 119-129. <https://doi.org/10.1007/s10344-015-0982-9>
- 11
12
13 557 Mañas, F., Gómez, A., Asensio, V., Palazón, S., Podra, M., Alarcia, O.E., Ruiz-Olmo, J., &
14 558 Casa, J. (2016b). Prevalence of antibody to aleutian mink disease virus in European mink
15 559 (*Mustela lutreola*) and american mink (*Neovison vison*) in Spain. *Journal of Wildlife Diseases*,
16 560 52, 22–32. <https://doi.org/10.7589/2015-04-082>
- 17
18
19 561 Maran, T., Skumatov, D., Gomez, A., Pödra, M., Abramov, A. V., & Dinets, V. (2016). *Mustela*
20 562 *lutreola*. The IUCN Red List of Threatened Species 2016. Retrieved from
21 563 <https://www.iucnredlist.org/species/14018/45199861>
- 22
23
24 564 Marchioni, E., & Berzero, G. (2015). Viral Infections of the Nervous System, In A. Sghirlanzoni,
25 565 G. Lauria, L. Chiapparini (Eds.), *Prognosis of Neurological Diseases*. (pp. 75-92) Milan, Italy:
26 566 Springer-Verlag Italia. <https://doi.org/10.1007/978-88-470-5755-5>
- 27
28
29 567 Melendez, L. V., Hunt, R. D., Daniel, M. D., Blake, B. J., & Garcia, F. G. (1971). Acute
30 568 lymphocytic leukemia in owl monkeys inoculated with herpesvirus saimiri. *Science*, 171, 1161–
31 569 1163. <https://doi.org/10.1126/science.171.3976.1161>
- 32
33
34 570 Miller, G., Shope, T., Coope, D., Waters, L., Pagano, J., Bornkamn, G., & Henle, W. (1977).
35 571 Lymphoma in cotton-top marmosets after inoculation with Epstein-Barr virus: tumor incidence,
36 572 histologic spectrum antibody responses, demonstration of viral DNA, and characterization of
37 573 viruses. *Journal of Experimental Medicine*, 145, 948–967. <https://doi.org/10.1084/jem.145.4.948>
- 38
39
40 574 Parkin, D. M. (2006). The global health burden of infection-associated cancers in the year 2002.
41 575 *International Journal of Cancer*, 118, 3030–3044. <https://doi.org/10.1002/ijc.21731>
- 42
43
44 576 Philippa, J., Fournier-Chambrillon, C., Fournier, P., Schaftenaar, W., van de Bildt, M., van
45 577 Herweijnen, R., Kuiken, T., Liabeuf, M., Ditcharry, S., Joubert, L., Bégner, M., & Osterhaus, A.
46 578 (2008). Serologic survey for selected viral pathogens in free-ranging endangered European mink
47 579 (*Mustela lutreola*) and other mustelids from south-western France. *Journal of Wildlife Diseases*,
48 580 44, 791–801. <https://doi.org/10.7589/0090-3558-44.4.791>

- 1
2
3 581 Quiroga, M. I., López-Peña, M., Vázquez, S., & Nieto, J. M. (1997). Distribution of Aujeszky's
4 582 disease virus in experimentally infected mink (*Mustela vison*). *Deutsche tierärztliche*
5 583 *Wochenschrift*, *104*, 147-150.
- 6
7
8 584 Ramer, J. C., Garber, R. L., Steele, K. E., Boyson, J. F., O'Rourke, C., & Thomson, J. A. (2000).
9 585 Fatal lymphoproliferative disease associated with a novel gammaherpesvirus in a captive
10 586 population of common marmosets. *Comparative Medicine*, *50*, 59-68.
- 11
12
13
14 587 Reading, M. J., & Field, H. J. (1999). Detection of high levels of canine herpes virus 1
15 588 neutralising antibody in kennel dogs using a novel serum neutralisation test. *Research in*
16 589 *Veterinary Science*, *66*, 273-275. <https://doi.org/10.1053/rvsc.1998.0222>
- 17
18
19 590 Reimer, D. C., & Lipscomb, T. P. (1998). Malignant seminoma with metastasis and herpesvirus
20 591 infection in a free-living sea otter (*Enhydra lutris*). *Journal of Zoo and Wildlife Medicine*, *29*, 35-
21 592 39.
- 22
23
24 593 Roizmann, B., Desrosiers, R. C., Fleckenstein, B., Lopez, C., Minson, A. C., & Studdert, M. J.
25 594 (1992). The family *Herpesviridae*: an update. *Archives of Virology*, *123*, 425-449.
26 595 <https://doi.org/10.1007/bf01317276>
- 27
28
29 596 Ryner, M., Strömberg, J. O., Söderberg-Nauclér, C., & Homman-Loudiyi, M. (2006).
30 597 Identification and classification of human cytomegalovirus capsids in textured electron
31 598 micrographs using deformed template matching. *Virology Journal*, *3*, 57.
32 599 <https://doi.org/10.1186/1743-422X-3-57>
- 33
34
35 600 Shannon-Lowe, C., Rickinson, A. B., & Bell, A. I. (2017). Epstein-Barr virus-associated
36 601 lymphomas. *Philosophical Transactions of the Royal Society B*, *372*, 20160271.
37 602 <https://doi.org/10.1098/rstb.2016.0271>
- 38
39
40 603 Siddle, H. V., Kreiss, A., Eldridge, M. D., Noonan, E., Clarke, C. J., Pyecroft, S., Woods, G. M.,
41 604 & Belov, K. (2007). Transmission of a fatal clonal tumor by biting occurs due to depleted MHC
42 605 diversity in a threatened carnivorous marsupial. *Proceedings of the National Academy of*
43 606 *Sciences of the United States of America*, *104*, 16221-16226.
44 607 <https://doi.org/10.1073/pnas.0704580104>
- 45
46
47 608 Sin, Y. W., Annavi, G., Dugdale, H. L., Newman, C., Burke, T., & MacDonald, D. W. (2014).
48 609 Pathogen burden, co-infection and major histocompatibility complex variability in the European
49 610 badger (*Meles meles*). *Molecular Ecology*, *23*, 5072-5088. <https://doi.org/10.1111/mec.12917>.

- 1
2
3 611 Summers, B., Greisen, H., & Appel, M. J. (1984). Canine distemper encephalomyelitis: variation
4 with virus strain. *Journal of Comparative Pathology*, *94*, 65-75. [https://doi.org/10.1016/0021-](https://doi.org/10.1016/0021-9975(84)90009-4)
5 612 [9975\(84\)90009-4](https://doi.org/10.1016/0021-9975(84)90009-4)
6
7 613
8
9 614 Tseng, M., Fleetwood, M., Reed, A., Gill, V. A., Harris, R. K., Moeller, R. B., Lipscomb, T. P.,
10 615 Mazet, J. A., & Goldstein, T. (2012). Mustelid Herpesvirus-2, a novel herpes infection in
11 616 northern sea otters (*Enhydra lutris kenyoni*). *Journal of Wildlife Diseases*, *48*, 181–185.
12 617 <https://doi.org/10.7589/0090-3558-48.1.181>
13
14 618 Tso, F. Y., Sawyer, A., Kwon, E. H., Mudenda, V., Langford, D., Zhou, Y., West, J., & Wood,
15 619 C. (2016). Kaposi's Sarcoma–Associated Herpesvirus Infection of Neurons in HIV-Positive
16 620 Patients. *The Journal of Infectious Diseases*, *215*, 1898-1907.
17 621 <https://doi.org/10.1093/infdis/jiw545>.
18
19 622 VanDevanter, D. R., Warrenner, P., Bennett, L., Schultz, E. R., Coulter, S., Garber, R. L., & Rose,
20 623 T. M. (1996). Detection and analysis of diverse herpesviral species by consensus primer PCR.
21 624 *Journal of Clinical Microbiology*, *34*, 1666–1671.
22
23 625 Venn-Watson, S., Benham, C., Gulland, F. M., Smith, C. R., St Leger, J., Yochem, P., Nollens,
24 626 H., Blas-Machado, U., Saliki, J., Colegrove, K., Wellehan, J. F. Jr., & Rivera, R. (2012). Clinical
25 627 relevance of novel Otarine herpesvirus-3 in California sea lions (*Zalophus californianus*):
26 628 Lymphoma, esophageal ulcers, and strandings. *Veterinary Research*, *43*, 85.
27 629 <https://doi.org/10.1186/1297-9716-43-85>
28
29 630 Wang, G., Du, Y., Wu, J. Q., Tian, F. L., Yu, X. J., & Wang, J. B. (2018). Vaccine resistant
30 631 pseudorabies virus causes mink infection in China. *BMC Veterinary Research*, *14*, 20.
31 632 <https://doi.org/10.1186/s12917-018-1334-2>
32
33 633 Widén, F., Das Neves, C. G., Ruiz-Fons, F., Reid, H. W., Kuiken, T., Gavier-Widén, D., &
34 634 Kaleta, E. F. (2012). *Herpesvirus Infections*. In D. Gavier-Widén, P. J. Duff, & A. Meredith.
35 635 (Eds.), *Infectious Diseases of Wild Mammals and Birds in Europe*. (pp. 3–36). Ames: Blackwell
36 636 Publishing Ltd. <https://doi.org/10.1002/9781118342442>
37
38
39
40
41
42
43
44
45
46
47
48
49
50
51
52
53
54
55
56
57
58
59
60

637 **Table 1.** Herpesviruses infections described in the family Mustelidae.

Species	HV name in the article	GenBank access n°.	Lesions attributable to herpesvirus	PCR prevalence	Tissue	Country	Author
European badger (<i>Meles meles</i>)	Mustelid herpesvirus 1 (MusHV-1, γ -HV)	AF376034 AY050215 AF275656	Cytopathic effect on badger' pulmonary fibroblasts	Single case	Pulmonary fibroblasts	UK	Banks et al. (2002)
	Mustelid herpesvirus-1 (MusHV-1, γ -HV)	Not provided	Not described	95% (18/19) 100% (10/10)	Blood Blood	UK Ireland	King et al. (2004)
	Mustelid herpesvirus-1 (MusHV-1, γ -HV)	GU799569	Not reported (detected in a road-kill animal)	Single case		Hungary	Dandár et al. (2010)
	Mustelid herpesvirus-1 (MusHV-1, γ -HV)	Not provided	Not described	98.1% (354/361)	Blood	UK	Sin et al. (2014)
	Mustelid gammaherpesvirus 1	AF275657	Not described	Single case	Lung	Not described	Unpublished
	Mustelid alphaherpesvirus 1	MF042164	Not described	Single case	Mediastinal lymph node	France	Unpublished
	Mustelid gammaherpesvirus-1 (MusGHV-1)	Not provided	Not detected	55% (54/98)	Genital swabs	UK	Kent et al. (2018)
Northern sea otter (<i>Enhydra lutris kenyoni</i>)	Mustelid herpesvirus-2 (MusHV-2, γ -HV)	GU979535	Presence of ulcers or pale raised plaques on the lingual, gingival, oral, esophageal and labial mucosa: epithelial hyperplasia and hyperkeratosis, often with epithelial cell degeneration and ulceration, and presence of eosinophilic intranuclear inclusion	46% (13/28)	Skin biopsies	United States	Tseng et al. (2012)

			bodies) Apparently healthy animal	34% (21/62)	nasal swabs	United States	
Oriental small-clawed otter (<i>Aonyx cinerea</i>)	Oriental small-clawed otter gammaherpesvirus (γ -HV)	FJ797657	Not described	Single case	Not described	Hungary	Unpublished
Captive fisher (<i>Martes pennanti</i>)	Fisher herpesvirus (FiHV, γ -HV)	HM579931	Multiple skin ulcers on the muzzle and plantar pads (thickened epidermis with increased numbers of koilocytes, perinuclear vacuolation, nuclear hypertrophy, pale amphophilic intranuclear inclusion bodies, and basophilic pseudoinclusions)	Single case	Skin ulcers	Born in captivity in the United States and sent to Canada	Gagnon et al. (2011)
American marten (<i>Martes americana</i>)	Marten alphaherpesvirus	KX062131 KX062132 KX062133	Not described	3 cases	Not described	Canada	Dalton et al. (2017)
	Marten betaherpesvirus	KX062129 KX062134 KX062135 KX062136	Not described	4 cases	Not described		
	Marten gammaherpesvirus 1	KX062128	Not described	2 cases	Not described		
	Marten gammaherpesvirus 2	KX062130					
European mink (<i>Mustela lutreola</i>)	Mustelid gammaherpesvirus-2	MN082678, MN082679	Basophilic (or eosinophilic, rarely found) inclusion bodies, and syncytia in a multifocal neural and perineural lymphoma.	8.7% (2/23)	Mediastinal B-cell lymphoma and lung	Spain	This work

1
2
3
4
5
6
7
8
9
10
11
12
13
14
15
16
17
18
19
20
21
22
23
24
25
26
27
28
29
30
31
32
33
34
35
36
37
38
39
40
41
42
43
44
45
46
47

638

Mustelid gammaherpesvirus-3	MN082680	Not detected	8.7% (2/23)	Oral swab, kidney, liver, spleen, bone marrow, brain, spinal cord, sciatic nerve and brachial plexus
--------------------------------	----------	--------------	-------------	---

For Peer Review Only

1
2
3 639 **FIGURES**
4

5 640

6 641 **Figure 1.** Maximum likelihood phylogram of the alignment of the obtained deduced amino
7 acid gammaherpesvirus sequences (marked with red dots) and other herpesvirus sequences
8 642 retrieved from GenBank. *Ictalurid herpesvirus 1* was selected as outgroup. The reliability of
9 643 the tree was tested by bootstrap analysis with 1,000 replicates, and those bootstrap values
10 644 lower than 70 were omitted.
11
12 645

13
14
15
16 646 **Figure 2.** Gross and microscopic findings in European mink (*Mustela lutreola*) PM-1: (A)
17 Periocular mass (white arrow). Scale bar = 1 centimeter. (B) Retrobulbar mass (right eye,
18 647 black arrow). Scale bar = 1 centimeter. (C) Perineural mass along the brachial plexus (black
19 648 arrows) and mediastinal mass (white arrow). Scale bar = 1 centimeter. (D) Mass effacing the
20 649 left adrenal gland (black arrow). (E) Note diffuse infiltration of neoplastic lymphocytes in the
21 650 perineural tissues and endoneurium of the brachial plexus mass; n = nerves (hematoxylin and
22 651 eosin). (F) Adrenal gland (a) is invaded by lymphoma (delimited with arrowheads)
23 652 (hematoxylin and eosin).
24
25 653
26
27
28
29
30

31 654 **Figure 3.** Microscopic and immunohistochemical findings in European mink (*Mustela*
32 *lutreola*) PM-1: (A) Higher magnification of endoneural (arrows) and perineural lymphoid
33 655 infiltrates in the brachial plexus mass. Note necrosis of neural tissue (asterisk). (B) A higher
34 656 magnification of neoplastic infiltrates demonstrates neoplastic lymphoblasts (hematoxylin and
35 657 eosin). (C) Note numerous basophilic intranuclear inclusion bodies (red arrowheads) in
36 658 unidentified cells and syncytia (black arrows) and few eosinophilic intranuclear inclusion
37 659 bodies surrounded by a clear halo (black arrowhead) in an area of necrosis involving a nerve
38 660 in the brachial plexus with perineural and neural lymphoma (hematoxylin and eosin). (D)
39 661 Lymphoma involving the spinal cord, particularly the pachymeninges (delimited with black
40 662 arrowheads) but also the white and grey matter (red arrowheads) (hematoxylin and eosin). (E)
41 663 Note positive immunolabeling for CD20 in perineural and endoneural neoplastic lymphocytes
42 664 in the brachial plexus mass. (F) Neoplastic lymphocytes are not labeled with CD3 antibodies.
43
44
45
46
47
48
49
50 665
51
52 666

53
54 667 **Figure 4.** Transmission electron microscopy (TEM) of the perineural lymphoma found in
55 668 European mink (*Mustela lutreola*) PM-1: (A) Intracytoplasmic herpesvirus-like particle (red

1
2
3
4 669 arrow) after nuclear egression but prior to acquiring the secondary envelopment in the
5 670 cytoplasm (which leads to the well-known enveloped herpesvirus particles seen on mature
6 671 virions) and nuclear membrane (yellow arrow). **(B)** Detailed view of the same particle (red
7
8
9 672 arrow) and nuclear membrane (yellow arrow).
10
11
12
13
14
15
16
17
18
19
20
21
22
23
24
25
26
27
28
29
30
31
32
33
34
35
36
37
38
39
40
41
42
43
44
45
46
47
48
49
50
51
52
53
54
55
56
57
58
59
60

For Peer Review Only

1
2
3 **1 Neoplasms and novel gammaherpesviruses in critically endangered captive European**
4 **2 minks (*Mustela lutreola*)**

5
6
7 **3 Running title: Neoplasms and gammaherpesviruses in European minks**
8

9
10 4 Olga Nicolas de Francisco¹, Fernando Esperón², Carles Juan-Sallés³, Ana Carolina Ewbank⁴,
11 5 Carlos G. das Neves⁵, Alberto Marco⁶, Elena Neves², Neil Anderson¹ and Carlos Sacristán^{2,4,*}
12
13

14 6 ¹The Royal (Dick) School of Veterinary Studies and the Roslin Institute, University of
15 7 Edinburgh, Roslin, EH25 9RG, UK.

16
17
18 8 ²Group of Epidemiology and Environmental Health, Animal Health Research Center (INIA-
19 9 CISA).Valdeolmos, Madrid, 28130, Spain.

20
21
22 10 ³Noah's Path, Elche, Alicante, 03203, Spain.

23
24
25 11 ⁴Laboratory of Wildlife Comparative Pathology, Department of Pathology, School of Veterinary
26 12 Medicine and Animal Sciences, University of São Paulo, São Paulo, SP, 05508-270, Brazil.

27
28
29 13 ⁵Norwegian Veterinary Institute. Oslo, PO Box 750 Sentrum, Norway.

30
31
32 14 ⁶Departament de Sanitat i d'Anatomia Animals, Facultat de Veterinària, Universitat Autònoma
33 15 de Barcelona (UAB), Bellaterra-Barcelona, 08193, Spain.
34
35
36
37
38

39 17 *Corresponding author: Carlos Sacristán, Laboratory of Wildlife Comparative Pathology,
40 18 Department of Pathology, School of Veterinary Medicine and Animal Sciences, University of
41 19 São Paulo, São Paulo, SP, Av. Prof. Dr. Orlando Marques de Paiva, 87, 05508-270, Brazil; Tel:
42 20 +55 11 981 121 073; Email: carlosvet.sac@gmail.com
43
44
45
46
47
48
49
50
51
52
53
54
55
56
57
58
59
60

21 SUMMARY

22 The European mink (*Mustela lutreola*) is a riparian mustelid, considered one of the most
23 endangered carnivores in the world. Alpha, beta, and gammaherpesviruses described in mustelids
24 have been occasionally associated with different pathological processes. However, there is no
25 information about the herpesviruses species infecting European minks. In this study, 141 samples
26 of swabs (oral, conjunctival, anal), feces and tissues from 23 animals were analyzed for
27 herpesvirus (HV) using a pan-HV PCR assay. Two different, potentially novel,
28 gammaherpesvirus species were identified in 12 samples from four animals (17.3%), and
29 tentatively named Mustelid gammaherpesvirus-2 (MUGHV-2) and MuGHV-3. Gross
30 examination was performed on dead minks (n=11), while histopathology was performed using
31 available samples from HV-positive individuals (n=2), identifying several neoplasms, including
32 B-cell lymphoma (identified by immunohistochemistry) with intralesional syncytia and
33 intranuclear inclusion bodies characteristic of HV (n=1), pulmonary adenocarcinoma (n=1), and
34 biliary (n=1) and preputial (n=1) cystadenoma, as well as other lesions (e.g., axonal vacuolar
35 degeneration [n=2] and neuritis [n=1]). Viral particles, consistent with HVs, were observed by
36 electron microscopy in the mink with neural lymphoma and inclusion bodies. This is the first
37 description of neoplasms and concurrent gammaherpesvirus infection in European minks. The
38 pathological, ultrastructural and PCR findings (MuGHV-2) in the European mink with
39 lymphoma strongly suggest a potential role for this novel gammaherpesvirus in its pathogenesis,
40 as it has been reported in other HV-infected species with lymphoma. The occurrence of neural
41 lymphoma with intralesional syncytia and herpesviral inclusions is, however, unique among
42 mammals. Further research is warranted to elucidate the potential oncogenic properties of
43 gammaherpesviruses in European mink, and their epidemiology in the wild population.

44 **Keywords:** biliary cystadenoma, herpesvirus, lymphoma, lung adenocarcinoma, mustelid,
45 preputial cystadenoma.

46 INTRODUCTION

47 The European mink (*Mustela lutreola*) is a critically endangered riparian mustelid with
48 populations in eastern (Ukraine, Russia, Estonia and Romania) and western (south-western
49 France and northern Spain) Europe (Maran et al., 2016). The main factors causing its decline are
50 interspecies competition with the non-native American mink (*Neovison vison*), habitat loss and
51 degradation (pollution), over-hunting, and infectious diseases (e.g., Aleutian mink disease and
52 canine distemper) (Lodé et al., 2001; Maran et al., 2016; Mañas et al., 2016a). Without the
53 implementation of more effective conservation measures, the European mink will very likely
54 soon become extinct in Spain (Ferrer, 2014).

55 To date, the exposure to, and infection by, several viruses have been studied in wild European
56 minks: *Aleutian mink disease virus* (Mañas et al., 2001; Fournier-Chambrillon et al., 2004;
57 Guzmán et al., 2008; Mañas et al., 2016b), *Canine morbillivirus* (syn. canine distemper virus)
58 (Mañas et al., 2001; Guzmán et al., 2008; Philippa et al., 2008), canine parainfluenza virus (syn.
59 parainfluenza virus type 5 or *Mammalian rubulavirus 5*), canine adenovirus (syn. *Canine*
60 *mastadenovirus A*), and viruses belonging to the families *Astroviridae*, *Picobirnaviridae*, and
61 *Parvoviridae* subfamily *Parvovirinae* (Bodewes et al., 2014). Nevertheless, in spite of the
62 numerous members of the family *Herpesviridae* of veterinary and public health significance
63 (Huff & Barry, 2003; Widén et al., 2012), to the authors' knowledge, there is no information
64 about herpesviruses (HVs) in European minks. The HVs infecting vertebrates (family
65 *Herpesviridae*) are further subdivided into three subfamilies: *Alphaherpesvirinae*,
66 *Betaherpesvirinae* and *Gammaherpesvirinae* (ICTV, 2017). In other mustelid species, for
67 example the sea otter (*Enhydra lutris*), HV-like intranuclear inclusion bodies along with HV-
68 compatible virions, and exposure to herpesvirus have been described (Reimer & Lipscomb,
69 1998; Goldstein et al., 2011). Alpha-, beta- and gammaherpesviruses (α -HVs, β -HVs, γ -HVs)
70 were identified in American martens (*Martes Americana*) with no mention to associated disease
71 (Dalton et al., 2017). Only γ -HV infection has been reported in other mustelids: in oral
72 ulcerations and plaques, and nasal secretions of sea otters (Tseng et al., 2012); in ulcerative skin
73 lesions of a captive fisher (*Martes pennanti*) (Gagnon et al., 2011); and in free-living European
74 badgers (*Meles meles*) (Banks et al., 2002; Dandár et al., 2010, Sin et al., 2014), in which a γ -HV
75 has not yet been associated with lesions or clinical disease (King et al., 2004). Finally, the
76 susceptibility to α -HV *Suid alphaherpesvirus 1*, the etiological agent of Aujeszky'

1
2
3 77 disease/pseudorabies (Gorham et al., 1998; Quiroga et al., 1997; Liu et al., 2017; Wang et al.,
4 78 2018) and the replication of α -HV *Canine herpesvirus-1* in fetal lung cells (Reading & Field,
5 79 1999) have been reported in American mink.

8
9 80 The goals of this study were to: (1) survey if HVs are present in a European mink captive
10 81 population; and (2) describe the clinical and pathological findings with a particular focus on
11 82 morphological evidence of an association with herpesviral infection.

14 83 **MATERIALS AND METHODS**

15 84 **Study population and samples**

16 85 This study was performed on the captive European mink population of the Pont de Suert Captive
17 86 Breeding Center (Pont de Suert, Lleida, northeastern Spain) which is part of the Spanish
18 87 Breeding Program. Ethical approval for this study was granted by the R(D)SVS Veterinary
19 88 Ethical Review Committee (VERC, process number 57.17) and the Government of Catalonia
20 89 (Wildlife and Plant Service within the Department of Sustainability and Territory).

21 90 The European mink samples were obtained from the live animal collection of the Pont de Suert
22 91 captive collection in September 2017 (identified as LM = live mink) and from the dead mink
23 92 stored at that center until October 2017 (identified as PM = postmortem mink). All these mink
24 93 were either originated from Spanish captive breeding centers or captured in the wild, also in
25 94 Spain. Individual sex, last weight, date and place of birth (when available), origin, and arrival
26 95 date to Pont de Suert, and date of death or euthanasia are summarized in Appendix 1. All
27 96 European minks in Pont de Suert tested negative for *Aleutian mink disease virus* and *Canine*
28 97 *morbillivirus* antibodies upon their admission to the captive breeding program.

29 98 In September 2017, all live adult European mink in the breeding center were anesthetized for
30 99 routine health check with a combination of intramuscular ketamine (5 mg/kg, Imalgene 100
31 100 mg/mL, Merial Laboratorios SA, Barcelona, Spain) and medetomidine (0.1 mg/kg, Domtor,
32 101 Ecuphar Veterinaria SLU, Barcelona, Spain). Intramuscular atipamezole (0.1 mg/kg, Antisedan,
33 102 Zoetis SLU, Madrid, Spain) was used to reverse the effects of medetomidine a minimum of 20
34 103 minutes after anesthesia had been induced. All animals were individually placed back into their
35 104 cages after sampling and full recovery. During anesthesia, all mink received a full clinical
36 105 examination by an experienced veterinarian, which included body condition assessment, skin and
37 106 hair inspection for ectoparasites, abdominal palpation and general examination of the mucosae,

1
2
3 107 oral cavity, ears, anal-genital region and feet, and cardiac and pulmonary auscultation.
4
5 108 Approximately 2 ml of blood were withdrawn by venipuncture from the cranial vena cava using
6
7 109 21-gauge 3.8-cm needles for hematology, biochemistry (data not shown), and molecular analysis
8
9 110 (0.5 mL in a sterile eppendorf). Aside from 0.5 mL of whole blood, sterile oropharyngeal,
10
11 111 conjunctival and anal swabs were also collected for molecular analysis, and preserved frozen at -
12
13 112 20 °C. Fresh fecal samples were taken from the cages using a sterile tube and refrigerated for
14
15 113 direct observation and egg flotation techniques with zinc sulphate (33%) for endoparasite
16
17 114 detection (data not shown) or frozen (-20 °C) to perform viral DNA detection.

17 115 **Molecular diagnostics**

18
19
20 116 A total of 141 frozen tissue samples from 23 European minks were analyzed by PCR for HV
21
22 117 detection. Anal and conjunctival swabs, blood, and feces from live mink (n=12) and
23
24 118 representative tissue samples from carcasses (n=10) (Appendix 2) were submitted for PCR
25
26 119 analysis. One additional animal was sampled while alive and after its death (codes LM-9 and
27
28 120 PM-9), thus included in both categories (live animal and carcasses, Appendix 2). After a lysis
29
30 121 step with lysis buffer (Cell Signaling Technology, MA, USA), DNA extraction was performed
31
32 122 by pressure filtration (QuickGene DNA tissue kit S, FujiFilm Life Science, Tokyo, Japan).
33
34 123 Initially, a mediastinal neoplastic tissue mass from PM-1 (index case) was analyzed by a nested
35
36 124 pan-PCR that amplified a fragment of approximately 215-315 bp of the HV DNA polymerase
37
38 125 gene (VanDevanter et al., 1996). A second PCR was performed to amplify a 500 bp fragment of
39
40 126 the HV glycoprotein B gene for gammaherpesviruses (Ehlers et al., 2008). In order to explore the
41
42 127 presence of the novel HV sequence obtained from the neoplastic tissue, a comprehensive HV
43
44 128 screening in tissues and samples from the captive breeding center (both live and dead animals)
45
46 129 was performed using the PCR described by Ehlers et al. (2008). All glycoprotein B gene-positive
47
48 130 samples were also tested for herpesviral DNA polymerase gene (VanDevanter et al., 1996).

49
50 131 The PCR products of DNA polymerase and glycoprotein B were visualized in 1.5% agarose gel
51
52 132 stained with Red Safe® (Ecogen, Spain), and the amplicons of expected size were directly
53
54 133 sequenced with sequencing primers TGVseq and IYGseq (DNA polymerase), and 2760s and
55
56 134 2761as (glycoprotein B), respectively described by VanDevanter et al. (1996) and Ehlers et al.
57
58 135 (2008). The obtained sequences were compared to those previously published in GenBank using
59
60 136 a Blast search, and nucleotide (nt) and deduced amino acid (aa) p-distances were calculated with

1
2
3 137 MEGA Software 7.0 after editing out the primers (Kumar et al., 2016). After ClustalW alignment
4
5 138 of glycoprotein B gene nucleotide sequences by MEGA software 7.0 (Kumar et al., 2016), nt and
6
7 139 aa maximum likelihood phylogenetic trees were generated with 1000 bootstrap replicates,
8
9 140 including the newly identified HV sequences and 39 other α -, β -, and γ -HVs sequences. *Ictalurid*
10
11 141 *herpesvirus 1* was selected as an outgroup. Sequence information for members of the
12
13 142 *Herpesviridae* family was obtained from GenBank.

14 143 **Gross and microscopic examination**

15
16 144 Complete postmortem gross examination was performed in eleven European mink (identified
17
18 145 with codes PM-1 through PM-11). Eight of them (PM-2 – PM-8, and PM-10) were prominently
19
20 146 autolyzed. Microscopic evaluation was performed on HV-PCR-positive animals with adequate
21
22 147 tissue preservation (PM-1 and PM-9), using 10% formalin-fixed tissues embedded in paraffin,
23
24 148 sectioned at 5 μ m-thick, and stained with hematoxylin and eosin.

25 149 **Immunohistochemistry**

26
27 150 Immunohistochemical analyses were performed in 4 μ m-thick paraffin wax-embedded tissue
28
29 151 samples of PM-1 using antibodies against CD20 and CD3. Briefly, slides were transferred to a
30
31 152 PT-Link Automatic System of DAKO for deparaffinization, rehydration and epitope retrieval.
32
33 153 For this last step, slides were treated with acid buffer at pH 6 for 20 min. at 98°C, and then
34
35 154 transferred to distilled water. Endogenous peroxidase was then inhibited with Peroxidase-
36
37 155 Blocking Solution (from Dako, Ref.: S2023). Immunostaining was performed on a Dako
38
39 156 Autostainer Plus, using procedures, buffers and solutions provided by the fabricant. Briefly, as
40
41 157 first antibody, a polyclonal Rabbit Anti- Human CD3 antibody (DAKO. Ref: A0452) and a
42
43 158 polyclonal Rabbit Anti- Human CD20 antibody (CULTEK. Ref: PA5-32313) were both
44
45 159 incubated for 40 min. at room temperature, diluted 1:100 (CD3) and 1:200 (CD20) in
46
47 160 EnVision™ FLEX buffer. After washing, the Rabbit/Mouse EnVision Detection System (Dako
48
49 161 Ref.: K5007) was incubated at room temperature for 40 min, at the dilution recommended by the
50
51 162 supplier. After washing, slides were incubated for 5 min. in DAB-Chromogen-hydrogen
52
53 163 peroxide (Dako K3468), to reveal binding. After washing, slides were counterstained in Mayer's
54
55 164 haematoxylin for 10 seconds, washed in running tap water, and then automatically dehydrated,
56
57 165 cleared and mounted.

58 166 **Electron microscopy**

1
2
3 167 Transmission electron microscopy (TEM) was performed in a paraffin-embedded sample of a
4
5 168 perineural mass found in PM-1. The tissue sample was deparaffinized with histoclear,
6
7 169 dehydrated with 100% ethanol, infiltrated with LRWhite, sectioned into 60 nm sections and
8
9 170 contrasted with uranylacetate. Micrographs were obtained using a FEI Morgagni 268
10
11 171 transmission electron microscope and images were recorded by a side-mounted Olympus Veleta
12
13 172 CCD charge-coupled device camera.

14 173 **RESULTS**

15 174 **Molecular study**

16
17
18 175 Herpesvirus DNA was detected in four (PM-1, PM-4, PM-8, and LM/PM-9) out of the 23
19
20 176 evaluated European minks. Positive HV amplification was observed in 8.5% (12/141) of the
21
22 177 analyzed samples, including 11 from postmortem tissue samples and one from an antemortem
23
24 178 oral swab (LM/PM-9) (Appendix 2).

25
26 179 Two different glycoprotein B gene sequences were detected in the four HV-positive European
27
28 180 mink; one sequence was amplified from PM-1 (mediastinal mass) and PM-8 (lung), and a
29
30 181 different one from PM-4 (liver, kidney, brain), and LM/PM-9 (an antemortem oral swab, brain,
31
32 182 spinal cord, peripheral nerve [sciatic nerve and brachial plexus], spleen, and bone marrow). The
33
34 183 nt and aa identities between both novel glycoprotein B sequences were 79.9% and 86.0%,
35
36 184 respectively. The first sequence, found in PM-1 and PM-8, was more similar to the sequence
37
38 185 detected in a European badger (MuGHV-1, GenBank Accession number: ABF15169) with,
39
40 186 correspondingly, nt and aa identities of 87.2% and 97.8%. The second sequence, found in PM-4
41
42 187 and LM/PM-9, was more related to *Lynx rufus* gammaherpesvirus-2 (ABF15169), with nt
43
44 188 identity of 78.4%, and had the highest aa identity (86.0%) with a γ -HV identified in a harp seal
45
46 189 (KP136799). A phylogenetic tree based on glycoprotein B amino acid deduced sequences
47
48 190 correctly classified the two obtained novel sequences within the cluster of terrestrial mammal γ -
49
50 191 HVs, genus *Percavirus*, with bootstrap values above 70% (Figure 1).

51
52 192 A DNA polymerase sequence was amplified in one of the four HV-positive animals (PM-1),
53
54 193 while no amplification for that gene was observed in the remaining glycoprotein B gene-positive
55
56 194 cases. The highest nt (86.5%) and aa (92.2%) identities of this sequence were to the fisher
57
58 195 gammaherpesvirus (HM579931) obtained in another mustelid species, the fisher. The DNA
59
60 196 polymerase sequence of PM-1 was submitted to GenBank database under accession number

1
2
3 197 MN082678, while the glycoprotein B sequences obtained from PM-1 and PM-9 were submitted
4
5 198 under accession numbers MN082679 and MN082680, respectively. Since there was a previous
6
7 199 report using the terms “Mustelid gammaherpesvirus” (Mustelid gammaherpesvirus-1 or
8
9 200 MuGHV-1, Kent et al. [2018]), we have tentatively named the two novel sequences as MuGHV-
10
11 201 2 (PM-1 and PM-8) and MuGHV-3 (PM-4 and LM/PM-9). A summary of the γ -HVs detected in
12
13 202 mustelids is provided in Table 1.

14 203 **Retrieval of information prior to death or euthanasia of HV-positive mink**

15
16 204 Prior to death, PM-1 presented with corneal opacity in the left eye, protrusion of right eye, severe
17
18 205 incoordination, and rear limb weakness, leading to traumatic lesions and inability to eat. PM-4
19
20 206 presented with poor fur quality and compromised vision. PM-8 was uncoordinated and
21
22 207 eventually recumbent, which lead to a skin ulcer on its right hip. LM/PM-9 presented with
23
24 208 corneal opacity in the left eye and bilateral impaired vision, mild incoordination, rear limbs
25
26 209 weakness, and hyporexia that progressed to anorexia. In order to prevent suffering and based on
27
28 210 a full clinical examination and complementary examinations (hematology and biochemistry, data
29
30 211 not shown), two old animals (over nine years of age; PM-1 and LM/PM-9) were humanely
31
32 212 euthanized due to the rapid worsening of clinical signs.

33 213 **Gross and microscopic findings**

34
35 214 The gross and histopathologic findings of the HV-positive mink (PM-1, PM-4, PM-8 and
36
37 215 LM/PM-9) are summarized in Appendix 3. The main gross and microscopic findings and
38
39 216 suspected cause of death in PM-1 and LM/PM-9 are described below.

40
41 217 PM-1 was a 647-grams male with moderate to severe atrophy of adipose tissue. Protrusion of the
42
43 218 right eye due to the presence of a grayish to greenish retrobulbar mass involving the eyelid and
44
45 219 peri-ocular skin (Figure 2). The left eye had corneal opacity. Nerves in the left brachial plexus
46
47 220 and left elbow joint nerves were surrounded by whitish masses up to 1 cm in greatest dimension
48
49 221 (Figure 2). A similar but smaller lesion surrounded the right sciatic nerve distal to the
50
51 222 coxofemoral joint. A 5.5x2.8x2.2-cm whitish mass was also found in the caudal mediastinum
52
53 223 (Figure 2). The left adrenal gland was partly effaced by a grayish mass 1 cm in diameter (Figure
54
55 224 2).

56
57 225 Microscopically, all masses consisted of a malignant neoplastic proliferation of round cells

1
2
3 226 characterized by a round, oval, or more rarely irregular, indented or reniform nucleus with 1-2
4
5 227 nucleoli and diverse chromatin patterns, and a low amount of eosinophilic to amphophilic
6
7 228 cytoplasm. Anisocytosis, anisokaryosis, and anaplasia were moderate to high, while
8
9 229 pleomorphism was moderate. Up to 6 mitoses per 40x power field were observed. Neoplastic
10
11 230 cells invaded the perineurium and endoneurium of nerves within the masses (Figures 2 and 3).
12
13 231 Affected nerves contained large areas of necrosis with dilatation, vacuolation and fragmentation
14
15 232 of myelin sheaths as well as spheroids, deposits of fibrin, infiltrates of neutrophils and
16
17 233 lymphocytes, and foci of acute hemorrhage. Neural necrosis extended into the perineural
18
19 234 neoplastic tissue, where it was accompanied by prominent infiltration of degenerate neutrophils.
20
21 235 Neoplastic cells were present in the perineurium and endoneurium as well. Intralesional within
22
23 236 the endoneurium and neoplastic tissue, particularly in areas of necrosis, were syncytia and
24
25 237 intranuclear inclusion bodies. These inclusions were predominantly basophilic and filled the
26
27 238 nucleus, but eosinophilic inclusions surrounded by a clear halo were noted as well (Figure 3).
28
29 239 They were found within syncytia and, presumably, neoplastic cells. Similar infiltrates of
30
31 240 neoplastic cells along with fewer well differentiated lymphocytes and plasma cells were present
32
33 241 in the spinal cord and root nerves, involving the meninges with a diffuse pattern and neural tissue
34
35 242 with a perivascular and multifocal distribution. In the spinal cord, both the white and grey matter
36
37 243 was affected (Figure 3). Cerebral meninges were also mildly infiltrated, but predominantly with
38
39 244 well differentiated lymphocytes and plasma cells; neoplastic round cells were rare in this
40
41 245 location. Neoplastic infiltrates in the retrobulbar mass and adrenal gland caused loss of
42
43 246 architecture (Figure 2) and invaded adjacent soft tissues including the skin, adipose tissue and
44
45 247 skeletal muscle. Thrombosis was observed in the right eyelid. Other microscopic findings were
46
47 248 cataracts in left eye, axonal degeneration in a peripheral skeletal muscle nerve, nodular acinar
48
49 249 pancreatic hyperplasia, prostatic hyperplasia, moderate glomerulosclerosis. Additional gross and
50
51 250 microscopic findings are summarized in Appendix 3.

52
53 251 PM-9 was a 696-grams male in a good body condition. This mink presented corneal opacity in
54
55 252 left eye, and mild thickening of the nictitating membrane. A marked bilateral hemothorax was
56
57 253 present, and both lungs were multifocally reddish in color. A mass 0.5 cm diameter was observed
58
59 254 in the diaphragmatic lobe of the left lung. This mink had mild to moderate splenomegaly, with a
60
255 red splenic mass of 0.5 cm in diameter. A cystic mass 1.5 in diameter was also noted in the left
256
liver lobe. A subcutaneous preputial mass measuring 1x0.5x0.3 cm, and mild generalized

1
2
3 257 lymphadenomegaly were also observed. The adrenal glands contained pale foci less than 1 mm
4
5 258 in diameter.

6
7 259 Microscopically, the main disease processes and lesions included pulmonary adenocarcinoma,
8
9 260 severe membranous glomerulonephritis, severe chronic diffuse granulomatous lymphadenitis,
10
11 261 biliary cystadenoma, and preputial gland cell hyperplasia and cystadenomas with focal malignant
12
13 262 transformation and purulent preputial adenitis. Other potential relevant lesions included
14
15 263 moderate to marked meningeal mineralization in the lumbar and thoracic spinal cord, mild
16
17 264 multifocal spongiosis in the brain, axonal vacuolar degeneration in the thoracic spinal cord and
18
19 265 sciatic nerve, as well as nodular hyperplasia of adrenocortical cells, pancreatic acinar and ductal
20
21 266 cells and splenic tissue, mild multifocal fibrosis and/or interstitial lymphoplasmacytic nephritis
22
23 267 and glomerulosclerosis. Other gross and microscopic findings are summarized in Appendix 3.

23 268 **Immunohistochemical findings**

24
25 269 Positive immunolabeling for the B cell marker CD20 was consistently observed in neoplastic
26
27 270 cells in the perineural masses and endoneurium of intra-tumoral nerves (Figure 3). Labeling most
28
29 271 notably involved the membrane. No labeling of neoplastic cells was observed for CD3 (Figure
30
31 272 3). Therefore, the lymphoma was classified as a B-cell lymphoma.

32 33 273 **Transmission electron microscopy (TEM)**

34
35 274 Transmission electron microscopy detected particles approximately 150 nm in diameter in the
36
37 275 perineural lymphoma identified in PM-1 (Figure 4). Some of these were similar to empty
38
39 276 nucleocapsids while others resembled nucleocapsids containing packaged DNA, and both were
40
41 277 compatible with herpesviral particles (Ryner et al., 2006).

42 43 278 **DISCUSSION**

44
45 279 Two different novel γ -HV sequences were identified in 12 samples from four unrelated adult
46
47 280 captive European mink (17.3%, 4/23) that, based on amino acid identities and phylogeny, could
48
49 281 be considered novel HV species (MuGHV-2 and MuGHV-3). The prevalence rate should be
50
51 282 interpreted with care, once no housekeeping genes were amplified to test the integrity of the
52
53 283 DNA present in the samples. This is, to the authors' knowledge, the first report of HV in
54
55 284 European mink, expanding the host range of HV infections in mustelids. Other γ -HV species
56
57 285 have been previously described in mustelids (King et al., 2004, Tseng et al., 2012, Dalton et al.,

1
2
3 286 2017), occasionally identified in lesions such as oral ulcerations and plaques (Tseng et al., 2012),
4
5 287 and skin ulcers (Gagnon et al., 2011). Nevertheless, this is the first description of γ -HV
6
7 288 potentially associated with neoplasms in mustelids.

8
9 289 The two γ -HV-infected European minks with available tissues for histopathology (PM-1 and
10
11 290 LM/PM-9) had several neoplasms, including B-cell lymphoma (n=1), pulmonary
12
13 291 adenocarcinoma (n=1), biliary cystadenoma (n=1) and preputial cystadenoma (n=1). To the
14
15 292 authors' knowledge, these are the first neoplasms described in this species. Age and infectious
16
17 293 disease and inbreeding may have played a role in the development of neoplasm. The influence of
18
19 294 other factors that may also be implicated, such as environmental contamination or inbreeding,
20
21 295 was not assessed. In other carnivore species, for instance the California sea lion (*Zalophus*
22
23 296 *californianus*), collaborative studies showed that certain neoplasms (urogenital carcinoma) were
24
25 297 associated with genotype, but also with HV and persistent organic pollutants (King et al., 2002;
26
27 298 Browning et al., 2015).

28
29 299 In regard to age, both animals with neoplasms and HV-infection (PM-1 and LM/PM-9) were
30
31 300 considered to be of advanced age for the species (over nine years old). The oldest recorded free-
32
33 301 ranging European mink was five years old; however, captive animals can reach ten years of age
34
35 302 (Mañas et al., 2016a). The nodular acinar pancreatic hyperplasia, prostatic hyperplasia and
36
37 303 glomerulosclerosis observed in PM-1, as well as nodular acinar and ductal pancreatic
38
39 304 hyperplasia, and nodular splenic hyperplasia in LM/PM-9 were possibly related to aging. Aging
40
41 305 should be considered an immunosuppression factor per se (Marchioni & Berzero, 2015), capable
42
43 306 of facilitating neoplasm development.

44
45 307 The European mink with neoplasms - PM-1 and LM/PM-9 – were infected with
46
47 308 gammaherpesviruses MuGHV-2 and MuGHV-3, respectively. HV-compatible particles were
48
49 309 observed by TEM in a B-cell lymphoma with neural tissue tropism of PM-1, in which
50
51 310 intratumoral syncytia and intranuclear inclusion bodies characteristic of herpesviruses were
52
53 311 noted. Noteworthy, viruses have been associated with approximately 15% to 20% of human
54
55 312 cancers worldwide (Parkin et al., 2006; Boccardo & Villa, 2007). Several γ -HV are oncogenic
56
57 313 viruses. For instance, Epstein–Barr virus (*Human gammaherpesvirus 4*) has been etiologically
58
59 314 associated with a broad range of lymphoproliferative lesions and B-, T- and NK-cell malignant
60
315 lymphomas in humans (Shannon-Lowe et al., 2017), including B-cell lymphoma in elderly

1
2
3 316 populations, possibly associated with immunosuppression due to aging (El Jamal, 2014; Castillo
4 317 et al., 2016). Kaposi sarcoma-associated HV (syn. *Human gammaherpesvirus 8*) is associated
5 318 with Kaposi's sarcoma and lymphoproliferative disorders in humans (Du et al., 2007). In wild
6 319 mammals, γ -HVs have been implicated in the pathogenesis of several neoplastic diseases,
7 320 including urogenital carcinoma or multicentric B-cell lymphoblastic lymphoma in California sea
8 321 lion (Lipscomb et al., 2000; Venn-Watson et al., 2012; Browning et al., 2015).
9 322 Gammaherpesvirus-associated lymphoproliferative disease has been observed in captive non-
10 323 human primates of the family Callitrichidae (Ramer et al., 2000). The experimental inoculation
11 324 of γ -HV saimiri herpesvirus in three-striped night monkeys (*Aotus trivirgatus*) induced acute
12 325 lymphocytic leukemia (Melendez et al., 1971), while Epstein-Barr virus inoculation caused
13 326 lymphoma in cotton-top tamarins (*Saguinus oedipus*) (Miller et al., 1977). The herpesviruses
14 327 identified in both mink, particularly in PM-1, may have been involved in the etiopathogenesis of
15 328 the neoplasms found. Conversely, the detection of γ -HVs in several tissues from infected animals
16 329 presenting neoplasms could have been caused by viral reactivation from latency, triggered by,
17 330 among other causes, immunosuppression (which could be associated with the presence of
18 331 neoplasms), given that γ -HVs become latent in lymphoid cells (Roizmann et al., 1992).
19 332 In the domestic ferret, a species closely related to the European mink, lymphomas are common
20 333 spontaneous malignancies. Healthy ferrets experimentally inoculated with non-cellular extracts
21 334 from ferrets with lymphoma also developed this neoplasm, which reinforces the potential role of
22 335 infectious agents in the horizontal transmission of lymphomas in this species (Erdman et al.,
23 336 1995). The role of *Aleutian mink disease virus* and retrovirus infection has been suggested
24 337 (Erdman et al., 1992). Unfortunately, due to economic constraints, the potential role of
25 338 retroviruses in European minks has not been assessed yet.
26 339 Inbreeding is another factor that could partially explain the observed neoplasms. The French and
27 340 Spanish European minks appear to be highly inbred (Maran et al., 2016), and it would be
28 341 interesting to know if these highly genetically uniform populations are more prone to neoplasia.
29 342 For instance, the loss or lack of major histocompatibility complex (MHC) diversity, known to
30 343 reduce immune response effectiveness, is postulated to contribute to the successful spread of the
31 344 devil facial tumour disease of Tasmanian devils (*Sarcophilus harrisi*) (Siddle et al., 2007). The
32 345 association between neoplasm (urogenital carcinoma) and inbreeding has also been identified in
33 346 California sea lion (Acevedo-Whitehouse et al., 2003).

1
2
3 347 The neurological clinical signs – mainly incoordination and rear limb weakness, presented by
4
5 348 three of the four HV-positive animals (PM-1, PM-8, LM/PM-9, all over 9 years of age) were
6
7 349 initially considered typical signs of weakness or aging-related degenerative disorders. The
8
9 350 microscopic lesions described in the peripheral and central nervous systems of two of the
10
11 351 examined animals potentially explain the observed neurological signs: peripheral and central
12
13 352 nervous system B-cell lymphomas, axonal degeneration, and peripheral skeletal muscle nerves
14
15 353 axonal degeneration (PM-1), and brain spongiosis, and spinal cord and sciatic nerve axonal
16
17 354 vacuolar degeneration (LM/PM-9). The spongiosis and axonal degeneration observed in
18
19 355 LM/PM-9 could be associated with metabolic (e.g., renal encephalopathy) and/or toxic disorders.
20
21 356 Noteworthy, LM/PM-9 had severe glomerulonephritis, mild interstitial lymphoplasmacytic
22
23 357 nephritis, glomerulosclerosis and azotemia, with high urea (410 mg/dl) and creatinine levels
24
25 358 (1.44 mg/dl). These were elevated when compared with the reference values described in other
26
27 359 mustelid, the ferret: 11-42 mg/dl and 0.2-1 mg/dl, respectively (Carpenter & Marion, 2017) and
28
29 360 the remaining European minks analyzed in this study (data not shown), which could explain the
30
31 361 incoordination signs. No reference values are available for European mink.

32
33 362 Interestingly, the MuGHV-2 found in case PM-1 presented neural tissue tropism, with HV
34
35 363 particles observed in a perineural mass, and similarly, LM/PM-9 samples of brain, spinal cord,
36
37 364 peripheral nerve (sciatic nerve and brachial plexus) were positive to MuGHV-3. Both animals
38
39 365 had incoordination. The etiology of the neuritis in the B-cell lymphoma of PM-1 is unclear; it
40
41 366 could have been due to secondary inflammation associated with the local necrosis or a direct
42
43 367 response against herpesviral infection. Some γ -HVs have marked neurotropism, such as *Human*
44
45 368 *herpesvirus 4*/ Epstein–Barr virus and *Human herpesvirus 4*/Kaposi's sarcoma-associated HV
46
47 369 (KSHV) (El Jamal et al., 2014; Tso et al., 2016). For instance, Epstein–Barr virus has been
48
49 370 suggested to cause CNS damage by parainfectious and direct virus-related mechanisms in
50
51 371 humans (e.g., meningitis, encephalitis and lymphoma) (El Jamal et al., 2014). Thus, it is not
52
53 372 possible to exclude HVs as the potential causative agents of the nervous clinical signs observed
54
55 373 in these infected mink. Cataracts, corneal melanosis, focal granulomatous conjunctivitis in left
56
57 374 eye, and protrusion of and periocular mass around the right eye observed in PM-1 may have
58
59 375 contributed to its impaired vision. All mink were seronegative to two other viral agents that
60
376 could also cause neurological clinical signs and/or impaired vision: *Aleutian mink disease virus*
377 (Hadlow, 1982; Dyer et al., 2000), and canine distemper (Summers et al., 1984). Histopathologic

1
2
3 378 evidence of infection with *Toxoplasma gondii*, *Encephalitozoon* spp. or *Sarcocystis neurona* was
4
5 379 not observed.

6
7 380 One of the novel European mink γ -HVs (Mu-GHV3) was detected in an antemortem oral swab
8
9 381 (LM-9), suggesting that viral shedding occurs in infected European minks and, therefore, that
10
11 382 horizontal HV transmission through oral secretions could be possible. Such characteristic has
12
13 383 been previously identified in γ -HV viruses; Epstein–Barr virus is commonly transmitted via
14
15 384 saliva (Marchioni & Berzero, 2015), and other γ -HVs have been detected in sea otter oral
16
17 385 mucosal ulcers and plaques (Tseng 2012), and in oral tissue and swabs samples from northern
18
19 386 elephant seals (*Mirounga angustirostris*) (Goldstein et al., 2006). None of the mink in this study
20
21 387 has oral ulcers. Transmission can be enhanced in captivity as close confinement leads to a higher
22
23 388 contact rate between animals and stress-related immunosuppression (Tseng et al., 2012).
24
25 389 Interestingly, one of the infected European minks (LM/PM-9) had lesions compatible with
26
27 390 chronic stress (bilateral nodular hyperplasia of adrenocortical cells), which could reactivate latent
28
29 391 γ -HV in the lymphoid tissue (Roizmann et al., 1992; Lam et al., 2013).

30
31 392 Three of the HV-infected European minks were captured in the Ebro River basin (PM-4, PM-8
32
33 393 and LM/PM-9). The fourth one (PM-1) was born in Pont de Suert in 2006. Herpesvirus can cause
34
35 394 lifelong infections (Roizmann et al., 1992); therefore, it was not possible to establish if these
36
37 395 animals became infected during their stay in the captive breeding center (the virus was detected
38
39 396 when they had already been in captivity for several years) or already carried the virus when they
40
41 397 joined the collection. As several European mink conservation programs involving species
42
43 398 restoration and reintroduction use animals bred in captivity (Mañas et al., 2001), future studies
44
45 399 should investigate whether these HVs are present in wild European mink populations. Due to the
46
47 400 fact that several HV infections predispose the host to secondary bacterial infections (Cabello et
48
49 401 al., 2013), and considering the small size of the European mink population, the authors believe
50
51 402 that monitoring for these viruses should be considered when implementing conservation
52
53 403 strategies including translocations, as has been advised for other species, e.g., the Darwin's fox
54
55 404 (*Lycalopex fulvipes*) (Cabello et al., 2013).

51 405 **CONCLUSIONS**

52
53 406 This is the first report of HV in European minks. Four European minks were positive to one of
54
55 407 the two identified novel herpesviruses: *Mustelid gammaherpesvirus 2* (MuGHV-2) and *Mustelid*

1
2
3 408 *gamma*herpesvirus 3 (MuGHV-3). Several neoplasms, including B-cell lymphoma,
4
5 409 adenocarcinoma and biliary and preputial cystadenoma, as well as neurological signs, were
6
7 410 observed in some of the γ -HV-infected European minks. Aside from the B-cell lymphoma case
8
9 411 potentially associated with MuGHV-2, the relationship between γ -HV infection and the
10
11 412 remaining lesions is unclear.

12 413 This study contributes to the conservation of European minks by expanding the current
13
14 414 knowledge on the viral diseases affecting this species. Additional research is needed to establish
15
16 415 the prevalence of these novel γ -HVs in free-ranging European mink populations, and to
17
18 416 investigate their pathogenicity and the role of herpesvirus and other potential cofactors in the
19
20 417 neoplasms detected in this particular European mink captive breeding population. This
21
22 418 information will be critical to take more scientifically based decisions and adopt management
23
24 419 techniques for the conservation of this endangered species, as well as to determine if infected
25
26 420 captive bred European minks could be released into the wild without negatively impacting the
27
28 421 species' conservation.

28 422 **Acknowledgements**

29
30 423 We thank the Pont de Suert Captive Breeding Center staff for their assistance and for providing
31
32 424 data and audiovisual information on the studied animals and Lene C. Hermansen (Imaging
33
34 425 Center, Norwegian University of Life Sciences) for the TEM analysis. We also thank Francesc
35
36 426 Mañas (Department of Environment, Generalitat de Catalunya) and Madis Podra (European
37
38 427 Mink Association) for their support and interest in this project, and for providing the information
39
40 428 regarding the studied animals, and Francisco Fernandez Rivera, Head of the Environmental
41
42 429 management in Forestal Catalana, for authorizing this study. Ana Carolina Ewbank receives a
43
44 430 doctoral-fellowship from the São Paulo Research Foundation (FAPESP, process number
45
46 431 2018/20956-0). Carlos Sacristán is a recipient of a post-doctoral fellowship by the FAPESP
47
48 432 (process number 2018/25069-7). This study was funded by the Innovation Initiative Grant (IIG)
49
50 433 and by donors of the Edinburgh Fund (University of Edinburgh).

51 434 **Conflict of Interest Statement:** the authors declare no conflict of interest.

52 435 **Data Availability Statement:** The data that supports our findings are available in the manuscript
53
54 436 and in the supplementary material.

437 **REFERENCES**

- 438 Acevedo-Whitehouse, K., Gulland, F., Greig, D., & Amos, W. (2003). Inbreeding: disease
439 susceptibility in California sea lions. *Nature*, 422, 35. <https://doi.org/10.1038/422035a>
- 440 Banks, M., King, D. P., & Daniells, C. (2002). Partial characterization of a novel
441 gammaherpesvirus isolated from a European badger (*Meles meles*). *Journal of General Virology*,
442 83, 1325–1330. <https://doi.org/10.1099/0022-1317-83-6-1325>
- 443 Bodewes, R., Ruiz-Gonzalez, A., Schapendonk, C. M., van den Brand, J. M., Osterhaus, A.D., &
444 Smits, S. L. (2014). Viral metagenomic analysis of feces of wild small carnivores. *Virology*
445 *Journal*, 11, 89. <https://doi.org/10.1186/1743-422X-11-89>
- 446 Boccardo, E., & Villa, L. L. (2007). Viral origins of human cancer. *Current Medicinal*
447 *Chemistry*, 14, 2526–2539. doi: <https://doi.org/10.2174/092986707782023316>
- 448 Browning, H. M., Gulland, F. M. D., & Hammond, J. A. (2015). Common cancer in a wild
449 animal: the California sea lion (*Zalophus californianus*) as an emerging model for
450 carcinogenesis. *Philosophical Transactions of the Royal Society B*, 370, 1673.
451 <https://doi.org/10.1098/rstb.2014.0228>.
- 452 Cabello, J., Esperón, F., Napolitano, C., Hidalgo, E., Dávila, J. A., & Millán, J. (2013).
453 Molecular identification of a novel gammaherpesvirus in the endangered Darwin's fox
454 (*Lycalopex fulvipes*). *Journal of General Virology*, 94, 2745–2749.
455 <https://doi.org/10.1099/vir.0.057851-0>.
- 456 Carpenter, J. W., & Marion, C. (2017). *Exotic Animal Formulary* (5th ed.). Philadelphia, PA:
457 Saunders.
- 458 Castillo, J. J., Beltran, B. E., Miranda, R. N., Young, K. H., Chavez, J. C., & Sotomayor, E. M.
459 (2016). EBV-positive diffuse large B-cell lymphoma of the elderly: 2016 update on diagnosis,
460 risk-stratification, and management. *American Journal of Hematology*, 91, 529-537.
461 <https://doi.org/10.1002/ajh.24370>
- 462 Dalton, C. S., van de Rakt, K., Fahlman, Å., Ruckstuhl, K., Neuhaus, P., Popko, R., Kutz, S., &
463 van der Meer, F. (2017). Discovery of herpesviruses in Canadian wildlife. *Archives of Virology*,
464 162, 449-456

- 1
2
3 465 Dandár, E., Szabó, L., & Heltai, M. (2010). PCR screening of mammalian predators (Carnivora)
4 466 for adenoviruses and herpesviruses: the first detection of a mustelid herpesvirus in Hungary.
5 467 *Magyar Allatorvosok Lapja*, 132, 302-308.
- 6
7
8 468 Du, M. -Q., Bacon, C. M., & Isaacson, P. G. (2007). Kaposi sarcoma-associated
9 469 herpesvirus/human herpesvirus 8 and lymphoproliferative disorders. *Journal of Clinical*
10 470 *Pathology*, 60, 1350-1357.
- 11
12
13
14 471 Dyer, N. W., Ching, B., & Bloom, M. E. (2000). Nonsuppurative meningoencephalitis associated
15 472 with Aleutian mink disease parvovirus infection in ranch mink. *Journal of Veterinary Diagnostic*
16 473 *Investigation*, 12, 159–162. <https://doi.org/10.1177/104063870001200212>
- 17
18
19
20 474 Ehlers, B., Dural, G., Yasmum, N., Lembo, T., de Thoisy, B., Ryser-Degiorgis, M. P., Ulrich, R.
21 475 G., & McGeoch, D. J. (2008). Novel mammalian herpesviruses and lineages within the
22 476 Gammaherpesvirinae: cospeciation and interspecies transfer. *Journal of Virology*, 82, 3509–
23 477 3516. <https://doi.org/10.1128/JVI.02646-07>.
- 24
25
26
27 478 El Jamal, S., Li, S., Bajaj, R., Wang, Z., Kenyon, L., Glass, J., Pang, C.S., Bhagavathi, S.,
28 479 Peiper, S. C., & Gong, J. Z. (2014). Primary central nervous system Epstein–Barr virus-positive
29 480 diffuse large B-cell lymphoma of the elderly: a clinicopathologic study of five cases. *Brain*
30 481 *Tumor Pathology*, 31, 265–273. <https://doi.org/10.1007/s10014-013-0173-x>
- 31
32
33
34 482 Erdman, S. E., Moore, F. M., Rose, F. M., & Fox, J. G. (1992). Malignant lymphoma in ferrets:
35 483 clinical and pathological findings in 19 cases. *Journal of Comparative Pathology*, 106, 37–47.
36 484 [https://doi.org/10.1016/0021-9975\(92\)90066-4](https://doi.org/10.1016/0021-9975(92)90066-4)
- 37
38
39
40 485 Erdman, S. E., Reimann, K. A., Moore, F. M., Kanki, P. J., Yu, Q. C., & Fox, J. G. (1995).
41 486 Transmission of a chronic lymphoproliferative syndrome in ferrets. *Laboratory Investigation; a*
42 487 *Journal of Technical Methods and Pathology*, 72, 539-546.
- 43
44
45 488 Ferrer, M. (2014). Life Lutreola Spain (2014-2018). Retrieved from
46 489 [http://ec.europa.eu/environment/life/project/Projects/index.cfm?fuseaction=search.dspPage&n_p](http://ec.europa.eu/environment/life/project/Projects/index.cfm?fuseaction=search.dspPage&n_proj_id=4908)
47 490 [roj_id=4908](http://ec.europa.eu/environment/life/project/Projects/index.cfm?fuseaction=search.dspPage&n_proj_id=4908)
- 48
49
50
51 491 Fournier-Chambrillon, C., Aasted, B., Perrot, A., Pontier, D., Sauvage, F., Artois, M., Cassiède,
52 492 J. M., Chauby, X., Dal Molin, A., Simon, C., & Fournier, P. (2004). Antibodies to Aleutian mink
53 493 disease parvovirus in free-ranging European mink (*Mustela lutreola*) and other small carnivores

- 1
2
3 494 from southwestern France. *Journal of Wildlife Diseases*, 40, 394-402.
4
5 495 <https://doi.org/10.7589/0090-3558-40.3.394>
6
7 496 Gagnon, C. A., Tremblay, J., Larochelle, D., Music, N., & Tremblay, D. (2011). Identification of
8
9 497 a novel herpesvirus associated with cutaneous ulcers in a fisher (*Martes pennanti*). *Journal of*
10
11 498 *Veterinary Diagnostic Investigation*, 23, 986–990. <https://doi.org/10.1177/1040638711418615>.
12
13 499 Goldstein, T., Lowenstine, L. J., Lipscomb, T. P., Mazet, J. A., Novak, J., Stott, J. L., & Gulland,
14
15 500 F. M., (2006). Infection with a novel gammaherpesvirus in northern elephant seals (*Mirounga*
16
17 501 *angustirostris*). *Journal of Wildlife Diseases*, 42, 830–835. [https://doi.org/10.7589/0090-3558-](https://doi.org/10.7589/0090-3558-42.4.830)
18
19 502 [42.4.830](https://doi.org/10.7589/0090-3558-42.4.830)
20
21 503 Goldstein, T., Gill, V. A., Tuomi, P., Monson, D., Burdin, A., Conrad, P. A., Dunn, J. L., Field,
22
23 504 C., Johnson, C., Jessup, D. A., Bodkin, J., & Doroff, A. M. (2011). Assessment of clinical
24
25 505 pathology and pathogen exposure in sea otters (*Enhydra lutris*) bordering the threatened
26
27 506 population in Alaska. *Journal of Wildlife Diseases*, 47, 579-592. [https://doi.org/10.7589/0090-](https://doi.org/10.7589/0090-3558-47.3.579)
28
29 507 [3558-47.3.579](https://doi.org/10.7589/0090-3558-47.3.579)
30
31 508 Gorham, J. R., Hartsough, G. R., & Burger, D. (1998). An epizootic of pseudorabies in ranch
32
33 509 mink. *Scientifur*, 22, 243-245.
34
35 510 Guzmán, D. S. M., Carvajal, A., García-Marín, J. F., Ferreras, M. C., Pérez, V., Mitchell, M.,
36
37 511 Urra, F., & Ceña, J. C. (2008). Aleutian disease serology, protein electrophoresis, and pathology
38
39 512 of the European mink (*Mustela lutreola*) from Navarra, Spain. *Journal of Zoo and Wildlife*
40
41 513 *Medicine*, 39, 305–313. <https://doi.org/10.1638/2006-0033.1>
42
43 514 Hadlow, W. J. (1982). Ocular lesions in mink affected with Aleutian disease. *Veterinary*
44
45 515 *Pathology*, 19, 5–15. <https://doi.org/10.1177/030098588201900103>
46
47 516 Huff, J. L., & Barry, P. A. (2003). B-Virus (*Cercopithecine herpesvirus 1*) infection in humans
48
49 517 and macaques: potential for zoonotic disease. *Emerging Infectious Diseases*, 9, 246-250.
50
51 518 <https://doi.org/10.3201/eid0902.020272>
52
53 519 ICTV (International Committee on Taxonomy of Viruses). (2017). Virus Taxonomy: The
54
55 520 Classification and Nomenclature of Viruses. Online (9th) Report of the ICTV. Email ratification
56
57 521 2017 (MSL #31). Retrieved from https://talk.ictvonline.org/ictv-reports/ictv_online_report/
58
59
60

- 1
2
3 522 Kent, A., Ehlers, B., Mendum, T., Newman, C., Macdonald, D. W., Chambers, M., & Buesching,
4 523 C. D. (2018). Genital tract screening finds widespread infection with Mustelid
5 524 Gammaherpesvirus 1 in the European badger (*Meles meles*). *Journal of Wildlife Diseases*, *54*,
6 525 133-137. <https://doi.org/10.7589/2016-12-274>
7
8
9
10 526 King, D. P., Hure, M. C., Goldstein, T., Aldridge, B. M., Gulland, F. M., Saliki, J. T., Buckles,
11 527 E. L., Lowenstine, L. J., & Stott, J. L. (2002). Otarine herpesvirus-1: a novel gammaherpesvirus
12 528 associated with urogenital carcinoma in California sea lions (*Zalophus californianus*). *Veterinary*
13 529 *Microbiology*, *86*, 131-137. [https://doi.org/10.1016/s0378-1135\(01\)00497-7](https://doi.org/10.1016/s0378-1135(01)00497-7)
14
15
16
17 530 King, D. R., Mutukwa, N., Lesellier, S., Cheeseman, C., Chambers, M. A., & Banks, M. (2004).
18 531 Detection of Mustelid herpesvirus-1 infected European badgers (*Meles meles*) in the British
19 532 Isles. *Journal of Wildlife Diseases*, *40*, 99–102. <https://doi.org/10.7589/0090-3558-40.1.99>
20
21
22
23 533 Kumar, S., Stecher, G., Tamura, K. (2016). MEGA7: Molecular Evolutionary Genetics Analysis
24 534 version 7.0 for bigger datasets. *Molecular Biology and Evolution*, *33*, 1870–1874.
25 535 <https://doi.org/10.1093/molbev/msw054>
26
27
28
29 536 Lam, L., Garner, M. M., Miller, C. L. (2013). A novel gammaherpesvirus found in oral
30 537 squamous cell carcinomas in sun bears (*Helarctos malayanus*). *Journal of Veterinary Diagnostic*
31 538 *Investigation*, *25*, 99–106.
32
33
34 539 Lipscomb, T. P., Scott, D. P., Garber, R. L., Krafft, A. E., Tsai, M. M., Lichy, J. H.,
35 540 Taubenberger, J. K., Schulman, F. Y., & Gulland, F. M. (2000). Common metastatic carcinoma
36 541 of California sea lions (*Zalophus californianus*): evidence of genital origin and association with
37 542 novel gammaherpesvirus. *Veterinary Pathology*, *37*, 609–617. [https://doi.org/10.1354/vp.37-6-](https://doi.org/10.1354/vp.37-6-609)
38 543 [609](https://doi.org/10.1354/vp.37-6-609)
39
40
41
42
43 544 Liu, H., Li, X. T., Hu, B., Deng, X. Y., Zhang, L., Lian, S. Z., Zhang, H. L., Lv, S., Xue, X. H.,
44 545 Lu, R. G., Shi, N., Yan, M. H., Xiao, P. P., & Yan, X. J. (2017). Outbreak of severe pseudorabies
45 546 virus infection in pig-offal-fed farmed mink in Liaoning Province, China. *Archives of Virology*,
46 547 *162*, 863-866. <https://doi.org/10.1007/s00705-016-3170-7>.
47
48
49
50 548 Lodé, T., Cormier, J. P., & Le Jacques, D. (2001). Decline in endangered species as an indication
51 549 of anthropic pressures: the case of European mink *Mustela lutreola* Western population.
52 550 *Environmental Management*, *28*, 727-735. <https://doi.org/10.1007/s002670010257>
53
54
55
56
57
58
59
60

- 1
2
3 551 Mañas, S., Ceña, J. C., Ruiz-Olmo, J., Palazón, S., Domingo, M., Wolfenbarger, J. B., & Bloom,
4 552 M. E. (2001). Aleutian mink disease parvovirus in wild riparian carnivores in Spain. *Journal of*
5 553 *Wildlife Diseases*, 37, 138-144. <https://doi.org/10.7589/0090-3558-37.1.138>
- 6
7
8 554 Mañas, S., Gómez, A., Asensio, V., Palazón, S., Pödra, M., Casal, J., & Ruiz-Olmo, J. (2016a).
9 555 Demographic structure of three riparian mustelid species in Spain. *European Journal of Wildlife*
10 556 *Research*, 62, 119-129. <https://doi.org/10.1007/s10344-015-0982-9>
- 11
12
13
14 557 Mañas, F., Gómez, A., Asensio, V., Palazón, S., Podra, M., Alarcia, O.E., Ruiz-Olmo, J., &
15 558 Casa, J. (2016b). Prevalence of antibody to aleutian mink disease virus in European mink
16 559 (*Mustela lutreola*) and american mink (*Neovison vison*) in Spain. *Journal of Wildlife Diseases*,
17 560 52, 22–32. <https://doi.org/10.7589/2015-04-082>
- 18
19
20
21 561 Maran, T., Skumatov, D., Gomez, A., Pödra, M., Abramov, A. V., & Dinets, V. (2016). *Mustela*
22 562 *lutreola*. The IUCN Red List of Threatened Species 2016. Retrieved from
23 563 <https://www.iucnredlist.org/species/14018/45199861>
- 24
25
26
27 564 Marchioni, E., & Berzero, G. (2015). Viral Infections of the Nervous System, In A. Sghirlanzoni,
28 565 G. Lauria, L. Chiapparini (Eds.), *Prognosis of Neurological Diseases*. (pp. 75-92) Milan, Italy:
29 566 Springer-Verlag Italia. <https://doi.org/10.1007/978-88-470-5755-5>
- 30
31
32
33 567 Melendez, L. V., Hunt, R. D., Daniel, M. D., Blake, B. J., & Garcia, F. G. (1971). Acute
34 568 lymphocytic leukemia in owl monkeys inoculated with herpesvirus saimiri. *Science*, 171, 1161–
35 569 1163. <https://doi.org/10.1126/science.171.3976.1161>
- 36
37
38 570 Miller, G., Shope, T., Coope, D., Waters, L., Pagano, J., Bornkamn, G., & Henle, W. (1977).
39 571 Lymphoma in cotton-top marmosets after inoculation with Epstein-Barr virus: tumor incidence,
40 572 histologic spectrum antibody responses, demonstration of viral DNA, and characterization of
41 573 viruses. *Journal of Experimental Medicine*, 145, 948–967. <https://doi.org/10.1084/jem.145.4.948>
- 42
43
44
45 574 Parkin, D. M. (2006). The global health burden of infection-associated cancers in the year 2002.
46 575 *International Journal of Cancer*, 118, 3030–3044. <https://doi.org/10.1002/ijc.21731>
- 47
48
49 576 Philippa, J., Fournier-Chambrillon, C., Fournier, P., Schaftenaar, W., van de Bildt, M., van
50 577 Herweijnen, R., Kuiken, T., Liabeuf, M., Ditcharry, S., Joubert, L., Bégner, M., & Osterhaus, A.
51 578 (2008). Serologic survey for selected viral pathogens in free-ranging endangered European mink
52 579 (*Mustela lutreola*) and other mustelids from south-western France. *Journal of Wildlife Diseases*,
53 580 44, 791–801. <https://doi.org/10.7589/0090-3558-44.4.791>

- 1
2
3 581 Quiroga, M. I., López-Peña, M., Vázquez, S., & Nieto, J. M. (1997). Distribution of Aujeszky's
4 582 disease virus in experimentally infected mink (*Mustela vison*). *Deutsche tierärztliche*
5 583 *Wochenschrift*, *104*, 147-150.
- 6
7
8 584 Ramer, J. C., Garber, R. L., Steele, K. E., Boyson, J. F., O'Rourke, C., & Thomson, J. A. (2000).
9 585 Fatal lymphoproliferative disease associated with a novel gammaherpesvirus in a captive
10 586 population of common marmosets. *Comparative Medicine*, *50*, 59-68.
- 11
12
13 587 Reading, M. J., & Field, H. J. (1999). Detection of high levels of canine herpes virus 1
14 588 neutralising antibody in kennel dogs using a novel serum neutralisation test. *Research in*
15 589 *Veterinary Science*, *66*, 273-275. <https://doi.org/10.1053/rvsc.1998.0222>
- 16
17
18 590 Reimer, D. C., & Lipscomb, T. P. (1998). Malignant seminoma with metastasis and herpesvirus
19 591 infection in a free-living sea otter (*Enhydra lutris*). *Journal of Zoo and Wildlife Medicine*, *29*, 35-
20 592 39.
- 21
22
23 593 Roizmann, B., Desrosiers, R. C., Fleckenstein, B., Lopez, C., Minson, A. C., & Studdert, M. J.
24 594 (1992). The family *Herpesviridae*: an update. *Archives of Virology*, *123*, 425-449.
25 595 <https://doi.org/10.1007/bf01317276>
- 26
27
28 596 Ryner, M., Strömberg, J. O., Söderberg-Nauclér, C., & Homman-Loudiyi, M. (2006).
29 597 Identification and classification of human cytomegalovirus capsids in textured electron
30 598 micrographs using deformed template matching. *Virology Journal*, *3*, 57.
31 599 <https://doi.org/10.1186/1743-422X-3-57>
- 32
33
34 600 Shannon-Lowe, C., Rickinson, A. B., & Bell, A. I. (2017). Epstein-Barr virus-associated
35 601 lymphomas. *Philosophical Transactions of the Royal Society B*, *372*, 20160271.
36 602 <https://doi.org/10.1098/rstb.2016.0271>
- 37
38
39 603 Siddle, H. V., Kreiss, A., Eldridge, M. D., Noonan, E., Clarke, C. J., Pyecroft, S., Woods, G. M.,
40 604 & Belov, K. (2007). Transmission of a fatal clonal tumor by biting occurs due to depleted MHC
41 605 diversity in a threatened carnivorous marsupial. *Proceedings of the National Academy of*
42 606 *Sciences of the United States of America*, *104*, 16221-16226.
43 607 <https://doi.org/10.1073/pnas.0704580104>
- 44
45
46 608 Sin, Y. W., Annavi, G., Dugdale, H. L., Newman, C., Burke, T., & MacDonald, D. W. (2014).
47 609 Pathogen burden, co-infection and major histocompatibility complex variability in the European
48 610 badger (*Meles meles*). *Molecular Ecology*, *23*, 5072-5088. <https://doi.org/10.1111/mec.12917>.

- 1
2
3 611 Summers, B., Greisen, H., & Appel, M. J. (1984). Canine distemper encephalomyelitis: variation
4 612 with virus strain. *Journal of Comparative Pathology*, *94*, 65-75. [https://doi.org/10.1016/0021-](https://doi.org/10.1016/0021-9975(84)90009-4)
5 613 [9975\(84\)90009-4](https://doi.org/10.1016/0021-9975(84)90009-4)
6
7
8 614 Tseng, M., Fleetwood, M., Reed, A., Gill, V. A., Harris, R. K., Moeller, R. B., Lipscomb, T. P.,
9 615 Mazet, J. A., & Goldstein, T. (2012). Mustelid Herpesvirus-2, a novel herpes infection in
10 616 northern sea otters (*Enhydra lutris kenyoni*). *Journal of Wildlife Diseases*, *48*, 181–185.
11 617 <https://doi.org/10.7589/0090-3558-48.1.181>
12
13
14 618 Tso, F. Y., Sawyer, A., Kwon, E. H., Mudenda, V., Langford, D., Zhou, Y., West, J., & Wood,
15 619 C. (2016). Kaposi's Sarcoma–Associated Herpesvirus Infection of Neurons in HIV-Positive
16 620 Patients. *The Journal of Infectious Diseases*, *215*, 1898-1907.
17 621 <https://doi.org/10.1093/infdis/jiw545>.
18
19
20 622 VanDevanter, D. R., Warrenner, P., Bennett, L., Schultz, E. R., Coulter, S., Garber, R. L., & Rose,
21 623 T. M. (1996). Detection and analysis of diverse herpesviral species by consensus primer PCR.
22 624 *Journal of Clinical Microbiology*, *34*, 1666–1671.
23
24
25 625 Venn-Watson, S., Benham, C., Gulland, F. M., Smith, C. R., St Leger, J., Yochem, P., Nollens,
26 626 H., Blas-Machado, U., Saliki, J., Colegrove, K., Wellehan, J. F. Jr., & Rivera, R. (2012). Clinical
27 627 relevance of novel Otarine herpesvirus-3 in California sea lions (*Zalophus californianus*):
28 628 Lymphoma, esophageal ulcers, and strandings. *Veterinary Research*, *43*, 85.
29 629 <https://doi.org/10.1186/1297-9716-43-85>
30
31
32 630 Wang, G., Du, Y., Wu, J. Q., Tian, F. L., Yu, X. J., & Wang, J. B. (2018). Vaccine resistant
33 631 pseudorabies virus causes mink infection in China. *BMC Veterinary Research*, *14*, 20.
34 632 <https://doi.org/10.1186/s12917-018-1334-2>
35
36
37 633 Widén, F., Das Neves, C. G., Ruiz-Fons, F., Reid, H. W., Kuiken, T., Gavier-Widén, D., &
38 634 Kaleta, E. F. (2012). *Herpesvirus Infections*. In D. Gavier-Widén, P. J. Duff, & A. Meredith.
39 635 (Eds.), *Infectious Diseases of Wild Mammals and Birds in Europe*. (pp. 3–36). Ames: Blackwell
40 636 Publishing Ltd. <https://doi.org/10.1002/9781118342442>
41
42
43
44
45
46
47
48
49
50
51
52
53
54
55
56
57
58
59
60

637 **Table 1.** Herpesviruses infections described in the family Mustelidae.

Species	HV name in the article	GenBank access n°.	Lesions attributable to herpesvirus	PCR prevalence	Tissue	Country	Author
European badger (<i>Meles meles</i>)	Mustelid herpesvirus 1 (MusHV-1, γ -HV)	AF376034 AY050215 AF275656	Cytopathic effect on badger' pulmonary fibroblasts	Single case	Pulmonary fibroblasts	UK	Banks et al. (2002)
	Mustelid herpesvirus-1 (MusHV-1, γ -HV)	Not provided	Not described	95% (18/19) 100% (10/10)	Blood Blood	UK Ireland	King et al. (2004)
	Mustelid herpesvirus-1 (MusHV-1, γ -HV)	GU799569	Not reported (detected in a road-kill animal)	Single case		Hungary	Dandár et al. (2010)
	Mustelid herpesvirus-1 (MusHV-1, γ -HV)	Not provided	Not described	98.1% (354/361)	Blood	UK	Sin et al. (2014)
	Mustelid gammaherpesvirus 1	AF275657	Not described	Single case	Lung	Not described	Unpublished
	Mustelid alphaherpesvirus 1	MF042164	Not described	Single case	Mediastinal lymph node	France	Unpublished
	Mustelid gammaherpesvirus-1 (MusGHV-1)	Not provided	Not detected	55% (54/98)	Genital swabs	UK	Kent et al. (2018)
	Northern sea otter (<i>Enhydra lutris kenyoni</i>)	Mustelid herpesvirus-2 (MusHV-2, γ -HV)	GU979535	Presence of ulcers or pale raised plaques on the lingual, gingival, oral, esophageal and labial mucosa: epithelial hyperplasia and hyperkeratosis, often with epithelial cell degeneration and ulceration, and presence of eosinophilic intranuclear inclusion	46% (13/28)	Skin biopsies	United States

			bodies) Apparently healthy animal	34% (21/62)	nasal swabs	United States	
Oriental small-clawed otter (<i>Aonyx cinerea</i>)	Oriental small-clawed otter gammaherpesvirus (γ -HV)	FJ797657	Not described	Single case	Not described	Hungary	Unpublished
Captive fisher (<i>Martes pennanti</i>)	Fisher herpesvirus (FiHV, γ -HV)	HM579931	Multiple skin ulcers on the muzzle and plantar pads (thickened epidermis with increased numbers of koilocytes, perinuclear vacuolation, nuclear hypertrophy, pale amphophilic intranuclear inclusion bodies, and basophilic pseudoinclusions)	Single case	Skin ulcers	Born in captivity in the United States and sent to Canada	Gagnon et al. (2011)
American marten (<i>Martes americana</i>)	Marten alphaherpesvirus	KX062131 KX062132 KX062133	Not described	3 cases	Not described	Canada	Dalton et al. (2017)
	Marten betaherpesvirus	KX062129 KX062134 KX062135 KX062136	Not described	4 cases	Not described		
	Marten gammaherpesvirus 1	KX062128	Not described	2 cases	Not described		
	Marten gammaherpesvirus 2	KX062130					
European mink (<i>Mustela lutreola</i>)	Mustelid gammaherpesvirus-2	MN082678, MN082679	Basophilic (or eosinophilic, rarely found) inclusion bodies, and syncytia in a multifocal neural and perineural lymphoma.	8.7% (2/23)	Mediastinal B-cell lymphoma and lung	Spain	This work

1
2
3
4
5
6
7
8
9
10
11
12
13
14
15
16
17
18
19
20
21
22
23
24
25
26
27
28
29
30
31
32
33
34
35
36
37
38
39
40
41
42
43
44
45
46
47

638	Mustelid gammaherpesvirus-3	MN082680	Not detected	8.7% (2/23)	Oral swab, kidney, liver, spleen, bone marrow, brain, spinal cord, sciatic nerve and brachial plexus
-----	--------------------------------	----------	--------------	-------------	---

For Peer Review Only

1
2
3 **639 FIGURES**
4

5 640

6 641 **Figure 1.** Maximum likelihood phylogram of the alignment of the obtained deduced amino
7 acid gammaherpesvirus sequences (marked with red dots) and other herpesvirus sequences
8 642 retrieved from GenBank. *Ictalurid herpesvirus 1* was selected as outgroup. The reliability of
9 643 the tree was tested by bootstrap analysis with 1,000 replicates, and those bootstrap values
10 644 lower than 70 were omitted.
11
12 645

13
14
15
16 646 **Figure 2.** Gross and microscopic findings in European mink (*Mustela lutreola*) PM-1: **(A)**
17 Periocular mass (white arrow). Scale bar = 1 centimeter. **(B)** Retrobulbar mass (right eye,
18 647 black arrow). Scale bar = 1 centimeter. **(C)** Perineural mass along the brachial plexus (black
19 648 arrows) and mediastinal mass (white arrow). Scale bar = 1 centimeter. **(D)** Mass effacing the
20 649 left adrenal gland (black arrow). **(E)** Note diffuse infiltration of neoplastic lymphocytes in the
21 650 perineural tissues and endoneurium of the brachial plexus mass; n = nerves (hematoxylin and
22 651 eosin). **(F)** Adrenal gland (a) is invaded by lymphoma (delimited with arrowheads)
23 652 (hematoxylin and eosin).
24
25 653
26
27
28
29
30

31 654 **Figure 3.** Microscopic and immunohistochemical findings in European mink (*Mustela*
32 *lutreola*) PM-1: **(A)** Higher magnification of endoneural (arrows) and perineural lymphoid
33 655 infiltrates in the brachial plexus mass. Note necrosis of neural tissue (asterisk). **(B)** A higher
34 656 magnification of neoplastic infiltrates demonstrates neoplastic lymphoblasts (hematoxylin and
35 657 eosin). **(C)** Note numerous basophilic intranuclear inclusion bodies (red arrowheads) in
36 658 unidentified cells and syncytia (black arrows) and few eosinophilic intranuclear inclusion
37 659 bodies surrounded by a clear halo (black arrowhead) in an area of necrosis involving a nerve
38 660 in the brachial plexus with perineural and neural lymphoma (hematoxylin and eosin). **(D)**
39 661 Lymphoma involving the spinal cord, particularly the pachymeninges (delimited with black
40 662 arrowheads) but also the white and grey matter (red arrowheads) (hematoxylin and eosin). **(E)**
41 663 Note positive immunolabeling for CD20 in perineural and endoneural neoplastic lymphocytes
42 664 in the brachial plexus mass. **(F)** Neoplastic lymphocytes are not labeled with CD3 antibodies.
43
44
45
46
47
48
49
50 665
51 666
52
53

54 667 **Figure 4.** Transmission electron microscopy (TEM) of the perineural lymphoma found in
55 668 European mink (*Mustela lutreola*) PM-1: **(A)** Intracytoplasmic herpesvirus-like particle (red
56
57
58
59
60

1
2
3
4 669 arrow) after nuclear egression but prior to acquiring the secondary envelopment in the
5 670 cytoplasm (which leads to the well-known enveloped herpesvirus particles seen on mature
6 671 virions) and nuclear membrane (yellow arrow), **(B)** Detailed view of the same particle (red
7 672 arrow) and nuclear membrane (yellow arrow).

10
11
12
13
14
15
16
17
18
19
20
21
22
23
24
25
26
27
28
29
30
31
32
33
34
35
36
37
38
39
40
41
42
43
44
45
46
47
48
49
50
51
52
53
54
55
56
57
58
59
60

For Peer Review Only

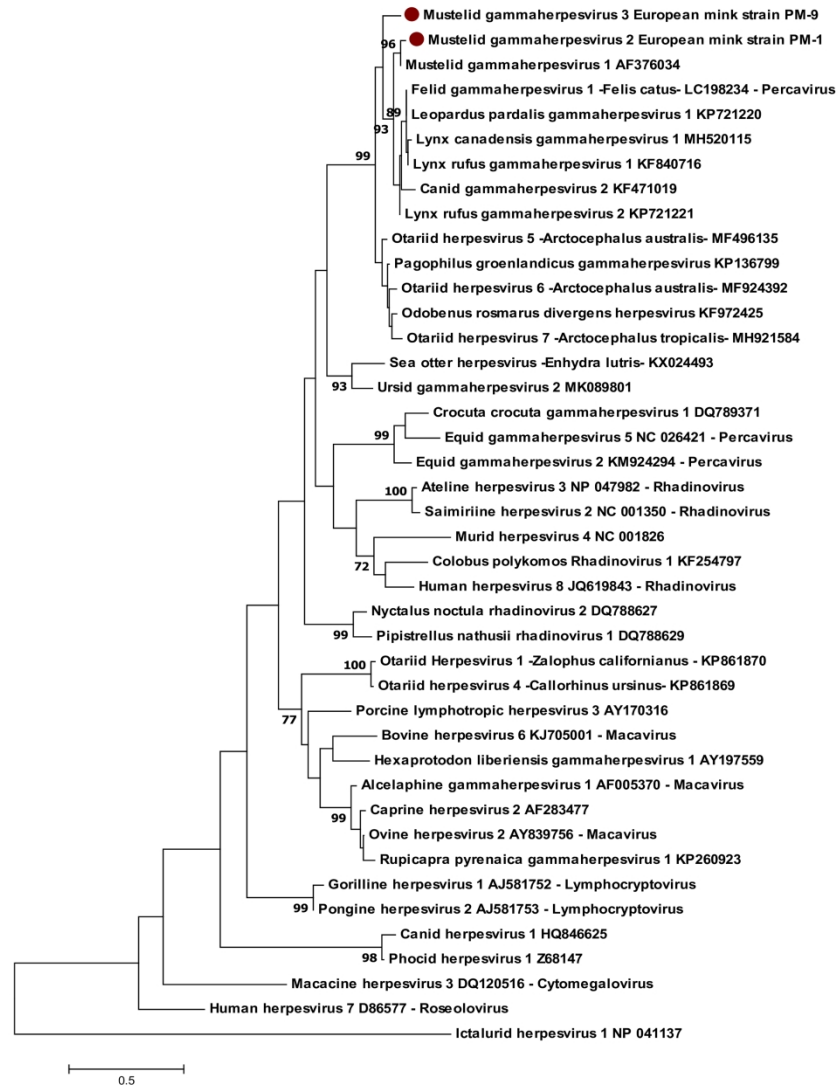


Figure 1. Maximum likelihood phylogram of the alignment of the obtained deduced amino acid gammaherpesvirus sequences (marked with red dots) and other herpesvirus sequences retrieved from GenBank. Ictalurid herpesvirus 1 was selected as outgroup. The reliability of the tree was tested by bootstrap analysis with 1,000 replicates, and those bootstrap values lower than 70 were omitted.

180x254mm (600 x 600 DPI)

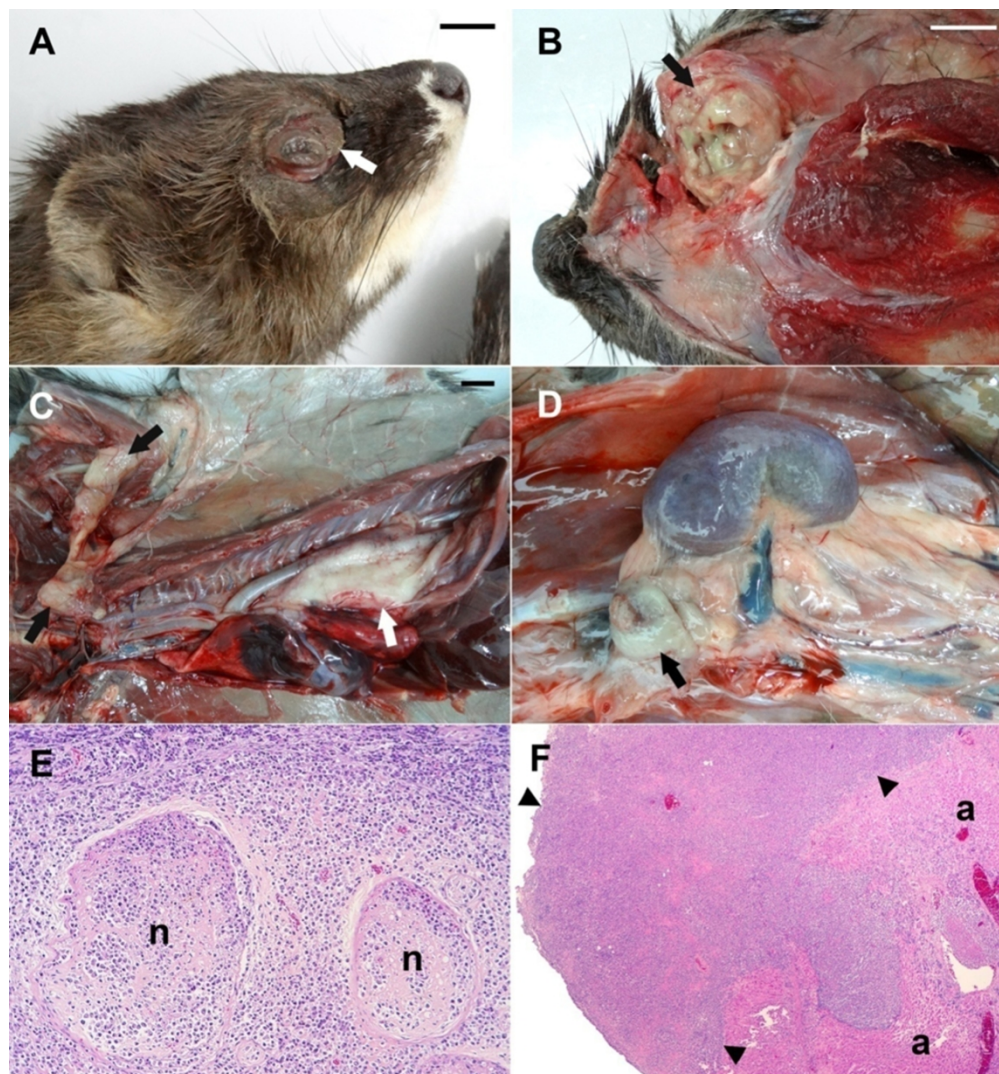


Figure 2. Gross and microscopic findings in European mink (*Mustela lutreola*) PM-1: (A) Periocular mass (white arrow). Scale bar = 1 centimeter. (B) Retrobulbar mass (right eye, black arrow). Scale bar = 1 centimeter. (C) Perineural mass along the brachial plexus (black arrows) and mediastinal mass (white arrow). Scale bar = 1 centimeter. (D) Mass effacing the left adrenal gland (black arrow). (E) Note diffuse infiltration of neoplastic lymphocytes in the perineural tissues and endoneurium of the brachial plexus mass; n = nerves (hematoxylin and eosin). (F) Adrenal gland (a) is invaded by lymphoma (delimited with arrowheads) (hematoxylin and eosin).

180x192mm (300 x 300 DPI)

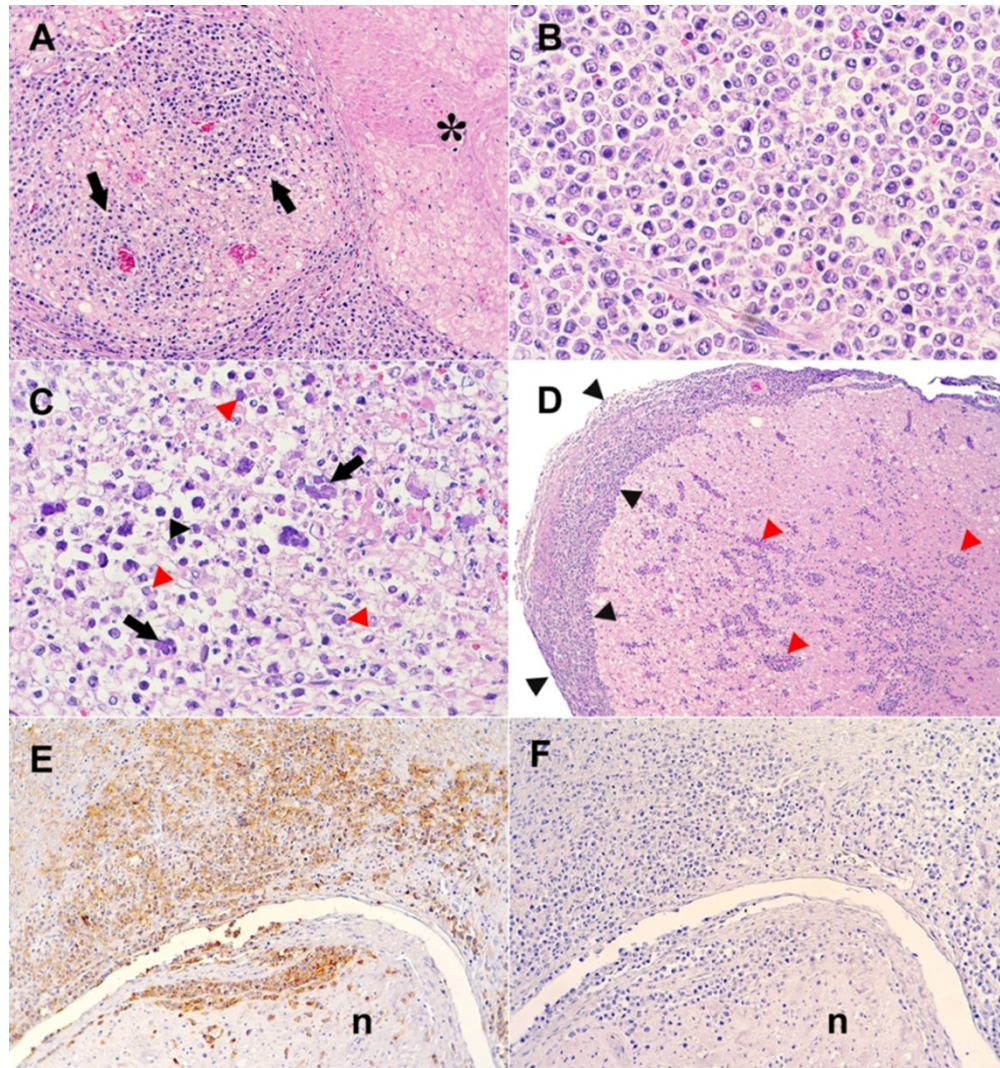


Figure 3. Microscopic and immunohistochemical findings in European mink (*Mustela lutreola*) PM-1: (A) Higher magnification of endoneural (arrows) and perineural lymphoid infiltrates in the brachial plexus mass. Note necrosis of neural tissue (asterisk). (B) A higher magnification of neoplastic infiltrates demonstrates neoplastic lymphoblasts (hematoxylin and eosin). (C) Note numerous basophilic intranuclear inclusion bodies (red arrowheads) in unidentified cells and syncytia (black arrows) and few eosinophilic intranuclear inclusion bodies surrounded by a clear halo (black arrowhead) in an area of necrosis involving a nerve in the brachial plexus with perineural and neural lymphoma (hematoxylin and eosin). (D) Lymphoma involving the spinal cord, particularly the pachymeninges (delimited with black arrowheads) but also the white and grey matter (red arrowheads) (hematoxylin and eosin). (E) Note positive immunolabeling for CD20 in perineural and endoneural neoplastic lymphocytes in the brachial plexus mass. (F) Neoplastic lymphocytes are not labeled with CD3 antibodies.

180x192mm (300 x 300 DPI)

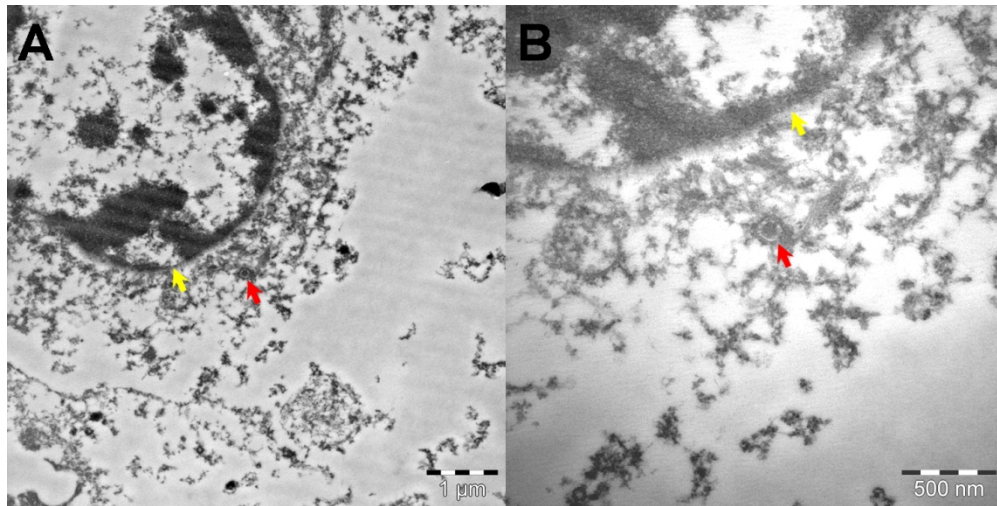


Figure 4. Transmission electron microscopy (TEM) of the perineural lymphoma found in European mink (*Mustela lutreola*) PM-1: (A) Intracytoplasmic herpesvirus-like particle (red arrow) after nuclear egression but prior to acquiring the secondary envelopment in the cytoplasm (which leads to the well-known enveloped herpesvirus particles seen on mature virions) and nuclear membrane (yellow arrow), (B) Detailed view of the same particle (red arrow) and nuclear membrane (yellow arrow).

125x62mm (300 x 300 DPI)

Table 1. Herpesviruses infections described in the family Mustelidae.

Species	HV name in the article	GenBank access n°.	Lesions attributable to herpesvirus	PCR prevalence	Tissue	Country	Author
European badger (<i>Meles meles</i>)	Mustelid herpesvirus 1 (MusHV-1, γ -HV)	AF376034 AY050215 AF275656	Cytopathic effect on badger' pulmonary fibroblasts	Single case	Pulmonary fibroblasts	UK	Banks et al. (2002)
	Mustelid herpesvirus-1 (MusHV-1, γ -HV)	Not provided	Not described	95% (18/19) 100% (10/10)	Blood Blood	UK Ireland	King et al. (2004)
	Mustelid herpesvirus-1 (MusHV-1, γ -HV)	GU799569	Not reported (detected in a road-kill animal)	Single case		Hungary	Dandár et al. (2010)
	Mustelid herpesvirus-1 (MusHV-1, γ -HV)	Not provided	Not described	98.1% (354/361)	Blood	UK	Sin et al. (2014)
	Mustelid gammaherpesvirus 1	AF275657	Not described	Single case	Lung	Not described	Unpublished
	Mustelid alphaherpesvirus 1	MF042164	Not described	Single case	Mediastinal lymph node	France	Unpublished
	Mustelid gammaherpesvirus-1 (MusGHV-1)	Not provided	Not detected	55% (54/98)	Genital swabs	UK	Kent et al. (2018)
Northern sea otter (<i>Enhydra lutris kenyoni</i>)	Mustelid herpesvirus-2 (MusHV-2, γ -HV)	GU979535	Presence of ulcers or pale raised plaques on the lingual, gingival, oral, esophageal and labial mucosa: epithelial hyperplasia and hyperkeratosis, often with epithelial cell	46% (13/28)	Skin biopsies	United States	Tseng et al. (2012)

			degeneration and ulceration, and presence of eosinophilic intranuclear inclusion bodies)	Apparently healthy animal	34% (21/62)	nasal swabs	United States	
Oriental small-clawed otter (<i>Aonyx cinerea</i>)	Oriental small-clawed otter gammaherpesvirus (γ -HV)	FJ797657	Not described	Single case	Not described	Hungary	Unpublished	
Captive fisher (<i>Martes pennanti</i>)	Fisher herpesvirus (FiHV, γ -HV)	HM579931	Multiple skin ulcers on the muzzle and plantar pads (thickened epidermis with increased numbers of koilocytes, perinuclear vacuolation, nuclear hypertrophy, pale amphophilic intranuclear inclusion bodies, and basophilic pseudoinclusions)	Single case	Skin ulcers	Born in captivity in the United States and sent to Canada	Gagnon et al. (2011)	
American marten (<i>Martes americana</i>)	Marten alphaherpesvirus	KX062131 KX062132 KX062133	Not described	3 cases	Not described	Canada	Dalton et al. (2017)	
	Marten betaherpesvirus	KX062129 KX062134 KX062135 KX062136	Not described	4 cases	Not described			

1
2
3
4
5
6
7
8
9
10
11
12
13
14
15
16
17
18
19
20
21
22
23
24
25
26
27
28
29
30
31
32
33
34
35
36
37
38
39
40
41
42
43
44
45
46

	Marten gammaherpesvirus 1	KX062128	Not described	2 cases	Not described		
	Marten gammaherpesvirus 2	KX062130					
European mink (<i>Mustela lutreola</i>)	Mustelid gammaherpesvirus-2	MN082678, MN082679	Basophilic (or eosinophilic, rarely found) inclusion bodies, and syncytia in a multifocal neural and perineural lymphoma.	8.7% (2/23)	Mediastinal B-cell lymphoma and lung	Spain	This work
	Mustelid gammaherpesvirus-3	MN082680	Not detected	8.7% (2/23)	Oral swab, kidney, liver, spleen, bone marrow, brain, spinal cord, sciatic nerve and brachial plexus		

For Peer Review Only

Appendix 1. History of all the European minks from Pont de Suert Captive Breeding Center evaluated in this study. NA= not applicable.

ID	Sex	Weight (grams)	Origin	Birth date	Year of arrival at Pont de Suert	Date of death/euthanasia
LM-1	F	566	Born in Pont de Suert	May 2011	2011	NA
LM-2	F	530	Born in Pont de Suert	May 2016	2016	NA
LM-3	F	618	Born in Pont de Suert	May 2015	2015	NA
LM-4	F	620	Born in Pont de Suert	May 2016	2016	NA
LM-5	F	555	Born in Pont de Suert	May 2014	2014	NA
LM-6	F	566	Born in Pont de Suert	May 2016	2016	NA
LM-7	M	780	Born in Pont de Suert	May 2015	2015	NA
LM-8	M	810	Born in Pont de Suert	May 2015	2015	NA
LM-9/PM-9	M	674	Captured in the wild	May-June 2008 [†]	2012	Oct 2017. Euthanasia
LM-10	M	740	Born in Pont de Suert	May 2013	2013	NA
LM-11	M	912	Captured in the wild	May-June 2015 [‡]	2017	NA
LM-12	M	760	Gipuzkoa captive center	May 2017	2017	NA
LM-13	F	594	Gipuzkoa captive center	June 2016	2017	NA
PM-1	M	960	Born in Pont de Suert	June 2006	Stayed in Captive center in Alava from 2006-2010. Went back to Pont de Suert in 2010	Oct 2015. Euthanasia
PM-2	F	394	Captured in the wild	Unknown	May 2004	Aug 2014. Death
PM-3	M	410	Alava captive center	May 2014	2014	End of 2014. Death
PM-4	F	350	Captured in the wild	Unknown	2004	Oct 2014. Died unexpectedly with no

							premonitory signs
PM-5	F	366	Born in Pont de Suert	May 2007	2007		Oct 2013. Death
PM-6	M	378	Born in Pont de Suert	May 2013	2013		Jul 2013. Death
PM-7	F	310	Born in Pont de Suert	June 2005	2005		Oct 2015. Death
PM-8	F	378	Captured in the wild	Unknown	2004		Jan 2014. Death
PM-10	M	990	Captured in the wild	2012	2015		Oct 2016. Died unexpectedly with no premonitory signs
PM-11	M	980	Born in Pont de Suert	June 2011	2011		Aug 2017. Death during transport

† The animal had to be euthanatized and was subsequently incorporated into the postmortem group with the identification “PM-9”. ‡Estimated data.

Appendix 2. Glycoprotein B sequences obtained from the analyzed samples. LM = Live mink. PM = postmortem mink.

ID	Sample number	Samples	HV-Sequence
LM-1	1	Anal swab	0
	2	Conjunctival swab	0
	3	Oral swab	0
	4	Feces	0
	5	Blood	0
LM-2	6	Anal swab	0
	7	Conjunctival swab	0
	8	Oral swab	0
	9	Feces	0
	10	Blood	0
LM-3	11	Anal swab	0
	12	Conjunctival swab	0
	13	Oral swab	0
	14	Feces	0
	15	Blood	0
LM-4	16	Anal swab	0
	17	Conjunctival swab	0
	18	Oral swab	0
	19	Feces	0
	20	Blood	0
LM-5	21	Anal swab	0
	22	Conjunctival swab	0
	23	Oral swab	0
	24	Feces	0
	25	Blood	0
LM-6	26	Anal swab	0
	27	Conjunctival swab	0
	28	Oral swab	0
	29	Feces	0
	30	Blood	0
LM-7	31	Anal swab	0
	32	Conjunctival swab	0
	33	Oral swab	0
	34	Feces	0
	35	Blood	0
LM-8	36	Anal swab	0
	37	Conjunctival swab	0
	38	Oral swab	0
	39	Feces	0
	40	Blood	0

1				
2				
3				
4		41	Anal swab	0
5		42	Conjunctival swab	0
6	LM-9†	43	Oral swab	1 (MuGHV-3)
7		44	Feces	0
8		45	Blood	0
9				
10		46	Anal swab	0
11		47	Conjunctival swab	0
12	LM-10	48	Oral swab	0
13		49	Feces	0
14		50	Blood	0
15				
16		51	Anal swab	0
17		52	Conjunctival swab	0
18	LM-11	53	Oral swab	0
19		54	Feces	0
20		55	Blood	0
21				
22				
23		56	Anal swab	0
24		57	Conjunctival swab	0
25	LM-12	58	Oral swab	0
26		59	Feces	0
27		60	Blood	0
28				
29		61	Anal swab	0
30		62	Conjunctival swab	0
31	LM-13	63	Oral swab	0
32		64	Feces	0
33		65	Blood	0
34				
35	PM-1	66	Mediastinal lymphoma	1 (MuGHV-2)
36				
37		67	Kidney	0
38		68	Lung	0
39		69	Liver	0
40	PM-2	70	Peripheral nerve	0
41		71	Spleen	0
42		72	Brain	0
43		73	Lymph node	0
44				
45				
46		74	Kidney	0
47		75	Lung	0
48		76	Liver	0
49	PM-3	77	Peripheral nerve	0
50		78	Spleen	0
51		79	Brain	0
52		80	Lymph node	0
53				
54				
55		81	Kidney	1 (MuGHV-3)
56		82	Lung	0
57	PM-4	83	Liver	1 (MuGHV-3)
58		84	Peripheral nerve	0
59		85	Spleen	0
60		86	Heart	0

1				
2				
3				
4		87	Ovary	0
5		88	Brain	1 (MuGHV-3)
6		89	Lymph node	0
7				
8		90	Kidney	0
9		91	Lung	0
10		92	Liver	0
11	PM-5	93	Peripheral nerve	0
12		94	Spleen	0
13		95	Ovary	0
14		96	Brain	0
15		97	Lymph node	0
16				
17		98	Kidney	0
18		99	Lung	0
19		100	Liver	0
20	PM-6	101	Peripheral nerve	0
21		102	Spleen	0
22		103	Brain	0
23		104	Lymph node	0
24				
25		105	Kidney	0
26		106	Lung	0
27		107	Liver	0
28		108	Peripheral nerve	0
29	PM-7	109	Spleen	0
30		110	Ovary	0
31		111	Brain	0
32		112	Lymph node	0
33				
34		113	Kidney	0
35		114	Lung	1 (MuGHV-2)
36		115	Liver	0
37		116	Peripheral nerve	0
38	PM-8	117	Spleen	0
39		118	Ovary	0
40		119	Brain	0
41		120	Lymph node	0
42				
43		121	Kidney	0
44		122	Brain	1 (MuGHV-3)
45		123	Liver	0
46		124	Spleen	1 (MuGHV-3)
47	PM-9 [†]	125	Bone marrow	1 (MuGHV-3)
48		126	Lymph node	0
49		127	Spinal cord	1 (MuGHV-3)
50		128	Peripheral nerve-sciatic nerve	1 (MuGHV-3)
51		129	Peripheral nerve-brachial plexus	1 (MuGHV-3)
52				
53		130	Spinal cord	0
54	PM-10	131	Lung	0
55		132	Peripheral nerve	0
56				
57				
58				
59				
60				

	133	Large intestine	0
	134	Muscle	0
	135	Liver	0
	136	Brain	0
	137	Cardiac blood	0
PM-11	138	Spinal cord	0
	139	Renal lymph node	0
	140	Spleen	0
	141	Kidney	0

† Samples of LM-9/PM-9 correspond to the same European mink; analyzed while alive and after his death.

For Peer Review Only

1 **Appendix 3.** Gross and microscopic findings (when available) of herpesvirus-positive animals (PM-1, PM-4, PM-8, PM-9).

ID	Tissue	Gross findings	Microscopic findings	HV
	Left eye	Corneal opacity	Severe cataracts; mild focal granulomatous conjunctivitis with intralesional vegetal matter; corneal melanosis	NA [†]
	Right eye	Ocular protrusion due a gray-greenish retrobulbar mass (2.5x2x2 cm) Light-tanned periocular mass (eyelid, 0.9x0.4x0.2 cm)	Perineural and neural lymphoma in the retrobulbar mass and the eyelid with invasion of skeletal muscle and skin and intralesional basophilic and rare eosinophilic intranuclear inclusion bodies surrounded by a clear halo and syncytia; severe necrotizing to necrosuppurative neuritis; eyelid thrombosis; foci of acute hemorrhage within the nerves	NA
	Meninges	NSFO [‡]	Lymphoplasmacytic infiltrate; rare neoplastic round cells	
	Brain	NSFO	NSFO	NA
	Spinal cord	NSFO	Lymphoma	NA
	Spinal nerves	NSFO	Lymphoma	NA
	Left brachial plexus, left elbow joint nerves, and right sciatic nerve	Light-tanned masses (5.5x1x1 cm mass on left brachial plexus and left elbow joint nerves; size of right sciatic nerve mass was not recorded)	Perineural and neural lymphoma with intralesional basophilic and rare eosinophilic intranuclear inclusion bodies surrounded by a clear halo and syncytia; severe necrotizing to necrosuppurative neuritis; foci of acute hemorrhage	NA
	Lungs	NSFO	NA	NA
	Heart	Concentric hypertrophy of left ventricle	NSFO	NA
	Mediastinum	Light tanned mass (5.5x2.8x2.2 cm) in the caudal mediastinum	Perineural and neural lymphoma with intralesional eosinophilic intranuclear basophilic (or eosinophilic, rarely found) inclusion bodies surrounded by a clear halo and syncytia; severe necrotizing to necrosuppurative neuritis; foci of acute hemorrhage within the nerves	MuGHV-2
	Peripheral skeletal muscle nerves	NSFO	Axonal degeneration	NA
	Unidentified lymph node	NSFO	Severe medullar sinus dilation with high protein lymph and blood resorption products	NA
	Stomach	Without contain	Lymphocytic ganglioneuritis	NA
	Intestines	NSFO	Mild to moderate diffuse lymphoplasmacytic eosinophilic enteritis, with presence of scarce neoplastic lymphoid cells	NA
	Liver	NSFO	Intrahepatocytic vacuoles with eosinophilic matter, and centrilobular distribution; severe hypertrophy and vacuolar degeneration of Ito cells	NA
	Spleen	NSFO	Mild extramedullary hematopoiesis	NA
	Pancreas	Several light tanned nodules, up to 2 mm in diameter	Moderate, multifocal, nodular, acinar hyperplasia	NA
PM-1	Prostate	NSFO	Prostatic hyperplasia; glandular ectasia; multifocal, interstitial neutrophilic lymphoplasmacytic prostatitis	NA

	Testicle	NSFO	Focal, acute, necrotizing mixed (neutrophilic and lymphohistocytic) arteritis; mild to moderate, multifocal tubular mineralization	NA
	Kidney	NSFO	Moderate glomerulosclerosis; mild polycystosis; mild multifocal tubular mineralization; and presence of hyaline cast within dilated tubules	NA
	Urinary bladder	NSFO	Leiomyositis; mild, multifocal, acute fibrinohemorrhagic cystitis with intramuscular mucin-rich edema	NA
	Skeletal muscle	NSFO	Non-inflammatory moderate multifocal sarcosporidiosis	NA
	Adipose tissue	Moderate to severe atrophy	Moderate, diffuse adipocyte atrophy	NA
	Adrenal gland	Light tanned mass (1 cm in diameter) involving left adrenal gland	Lymphoma with invasion of the adjacent adipose tissue	NA
	Brain	NSFO	NA	MuGHV-3
	Peripheral nerve	NSFO	NA	0
	Lung	Congestion	NA	0
	Heart	Hemopericardium	NA	0
	Kidney	NSFO	NA	MuGHV-3
	Liver	Congestion	NA	MuGHV-3
	Spleen	NSFO	NA	0
	Ovary	Left ovarian cyst (2 cm in diameter)	NA	0
	Lymph node	NSFO	NA	0
	Skin	Large ulceration on the lateral right femoral area	NA	NA
	Brain	NSFO	NA	0
	Peripheral nerve	NSFO	NA	0
	Lung	Congestion	NA	MuGHV-2
	Kidney	NSFO	NA	0
	Liver	Congestion	NA	0
	Spleen	NSFO	NA	0
	Lymph node	NSFO	NA	0
	Ovary	NSFO	NA	0
	Left eye	Corneal opacity, possible thickening of nictitating membrane	NA	NA
	Brain	NSFO	Mild multifocal spongiosis; mild, arterial (focal) and paquimeningeal mineralization	MuGHV-3
	Spinal cord	NSFO	Mild, multifocal axonal vacuolar degeneration associated with focal gliosis and moderate to marked multifocal meningeal mineralization	MuGHV-3
	Sciatic nerve	NSFO	Multifocal axonal vacuolar degeneration with intra-axonal basophilic inclusion bodies (Lafora bodies)	MuGHV-3

Brachial plexus	NSFO	Autolysis	MuGHV-3
Lymph nodes	Mild generalized lymphadenomegaly	Chronic, severe, diffuse granulomatous lymphadenitis; phagocytosis of silica crystals; intralesional mineralization. Second lymph node: chronic mild to moderate multifocal granulomatous lymphadenitis with medullar sinus dilatation	0
Heart	NSFO	Focal adventitial arterial mineralization	NA
Lungs	Reddish in color, presence of nodular mass (0.5 cm in diameter) in the diaphragmatic left lobe	Well-delimited nodular non-encapsulated adenocarcinoma; mild multifocal subpleural histiocytic and lymphocytic lipid pneumonia	NA
Stomach	Empty stomach	Mild multifocal neutrophilic and lymphoplasmacytic gastritis; multifocal luminal glandular neutrophilic casts	NA
Intestines	NSFO	Mild diffuse lymphoplasmacytic enteritis	NA
Liver	Left liver lobe cystic mass (1.5x1.5 cm)	Biliary cystadenoma; vacuolar degeneration of the Ito cells	0
Spleen	Mild to moderate splenomegaly, 0.5 cm in diameter nodular focal red mass	Nodular hyperplasia; mild diffuse extramedullary hematopoiesis; diffuse blood sequestration	MuGHV-3
Bone marrow	NSFO	Autolysis	MuHHV-3
Kidney	NSFO	Severe membranous glomerulonephritis with tubular dilatation, intratubular hyaline casts, mild multifocal fibrosis and/or interstitial lymphoplasmacytic nephritis and glomerulosclerosis, mild intratubular crystals phagocytized/surrounded by multinucleated giant cells. Tubular polycystosis, one of them associated with atrophy caused by perilesional compression	0
Skeletal muscle	NSFO	Non-inflammatory mild multifocal sarcosporidiosis	NA
Adrenal gland	Pale nodules (< 1 mm in diameter)	Bilateral diffuse nodular hyperplasia of cortical cells	NA
Thyroid gland	NSFO	Moderate nodular or diffuse hypertrophy (hyperplastic goiter)	NA
Parathyroid gland	NSFO	Mild to moderate hypertrophy and cytoplasmic vacuolization of chief cells	NA
Pancreas	NSFO	Mild multifocal nodular ductal hiperplasia; multifocal nodular acinar hyperplasia	NA
Prepuce	Subcutaneous reddish mass (1x0.5x0.3 cm)	Hyperplasia and cystadenomas of preputial glands with focal malignant transformation (to cystadenocarcinoma); purulent adenitis	NA
Testicle	NSFO	Bilateral diffuse atrophy of seminiferous tubules with possible fibrosis/hyalinization of tubular basement membrane; moderate bilateral multifocal mineralization of seminiferous tubules; mild intimal and medial arterial mineralization with mild intimal fibrosis (pampiniform plexus)	NA

2 † NA= not analyzed; *NSFO= no significant findings were observed.